GEOSPHERE

GEOSPHERE; v. 14, no. 2

doi:10.1130/GES01546.1

14 figures; 3 tables

CORRESPONDENCE: mikari@marum.de

CITATION: Ikari, M.J., Kopf, A.J., Hüpers, A., and Vogt, C., 2018, Lithologic control of frictional strength variations in subduction zone sediment inputs: Geosphere, v. 14, no. 2, p. 604–625, doi:10.1130/GES01546.1.

Science Editor: Shanaka de Silva
Guest Associate Editor: Philippe Agard

Recieved 20 April 2017
Revison received 16 November 2017
Accepted 31 January 2018
Published online 28 February 2018

Lithologic control of frictional strength variations in subduction zone sediment inputs

Matt J. Ikari, Achim J. Kopf, Andre Hüpers, and Christoph Vogt

MARUM Center for Marine Environmental Sciences and Faculty of Geosciences, University of Bremen, D-28359 Bremen, Germany

ABSTRACT

At convergent margins, marine sediments deposited seaward of the subduction zone forearc on the incoming plate (the "subduction inputs") represent the initial condition for geomechanical processes during subduction. The frictional strength of these sediments is a key parameter governing deformation during subduction, which is controlled to first order by lithologic composition. We combine here the results of laboratory friction experiments and quantification of mineral assemblage for scientific drilling samples recovered from three particularly well-studied subduction zones: the Nankai Trough (southwestern Japan), the Japan Trench (northeastern Japan), and Costa Rica. In the Japan Trench, frictionally weak smectite-rich pelagic clay contrasts sharply with stronger, more siliceous hemipelagic material. This strength contrast dictates the stratigraphic position of initial plate boundary formation and influences slip behavior of the shallow megathrust. In the Costa Rica subduction zone, relatively weak clay-rich hemipelagic sediment overlies frictionally strong pelagic nannofossil oozes and chalks, which could be a factor for the development of features such as a small amount of offscraping near the toe and subduction erosion where ooze or chalk dominates. In the Nankai Trough, however, a wide range of frictional strength values is observed that does not correlate with clay mineral content. In this case, mechanical behavior at Nankai is likely influenced by other factors related to diagenesis or fluid overpressuring.

INTRODUCTION

In subduction zones, a variety of fundamental processes and characteristics are controlled by the shear strength of geologic materials. This includes the shape and structure of the wedge, the development of incipient deformation, the slip behavior of shallow faults, and sediment mass transport. A wealth of laboratory work has established that the shear strength of geologic materials is dependent on the mineralogy or lithology to first-order degree (e.g., Summers and Byerlee, 1977; Byerlee, 1978; Shimamoto and Logan, 1981a, 1981b; Morrow et al., 2000; Brown et al., 2003; Ikari et al., 2009). The sedimentary section on the incoming plate (i.e., the "subduction inputs") represents the initial lithologic condition for all processes associated with eventual subduction, therefore it is crucial to characterize the lithology and mineralogy of the subduction inputs (Underwood, 2007).

In subduction zones, the plate boundary forms as a large-scale thrust fault (or "megathrust"), and other subsidiary faults such as splays and imbrications are hosted within the forearc. On the shallowest reaches of fault zones near the prism toe, slip behavior is heavily influenced by the host sediment and therefore the lithostratigraphy of the incoming plate. This is particularly important because coseismic slip that propagates to the seafloor is a major tsunami hazard (e.g., Polet and Kanamori, 2000; Ito et al., 2011). Nucleation of major earthquakes is less directly affected by the inputs due to the myriad of diagenetic and metamorphic effects on the sediment before reaching tens of kilometers in depth (Moore and Saffer, 2001; Moore et al., 2007).

Because fault zones are planes of weakness, they are expected to form where intrinsically weak sediments are found, or where pore pressures are elevated. Therefore, the position of the plate boundary décollement is controlled by the lithostratigraphy of the incoming plate. For several margins, it has been suggested that at the onset of subduction, the décollement preferentially localizes in weak strata (e.g., Moore, 1989; Deng and Underwood, 2001; Kopf and Brown, 2003). This is inferred from mechanical data, and often corroborated by seismic reflection data in which the plate boundary proto-décollement can be correlated with negative-polarity reflectors in the incoming sequence (e.g., MacKay, 1995; Moore et al., 1995, 1998; Costa Pisani et al., 2005).

Frictional strength also plays a role in controlling the large-scale shape of the wedge. In the simplest form of the Coulomb wedge model, the angle made by the slope of the seafloor and dip of the megathrust is controlled by the frictional strength of the megathrust interface and the internal strength of the wedge (Davis et al., 1983; Dahlen, 1990). If the wedge becomes oversteepened, its critical shape is maintained by deformation (faulting) within the wedge and may result in slope failure at the seafloor, e.g., in the form of submarine landslides or turbidites, which are common on the wedge (e.g., Adams, 1990; Goldfinger et al., 2000; von Huene et al., 2004; Strasser et al., 2011, 2012). Submarine landslides, which in many cases occur due to the presence of a weak layer in shallow strata (e.g., Masson et al., 2006), also occur in the subduction inputs (Kitamura and Yamamoto, 2012).

In this paper, we systematically review the relationship between mineral assemblage and frictional behavior for pre-subduction ocean sediments, focusing on three well-studied subduction zones: the Nankai Trough, Japan Trench, and Costa Rica. We then explore the implications of these relationships for subduction zone mechanics, specifically initiation of décollement formation.

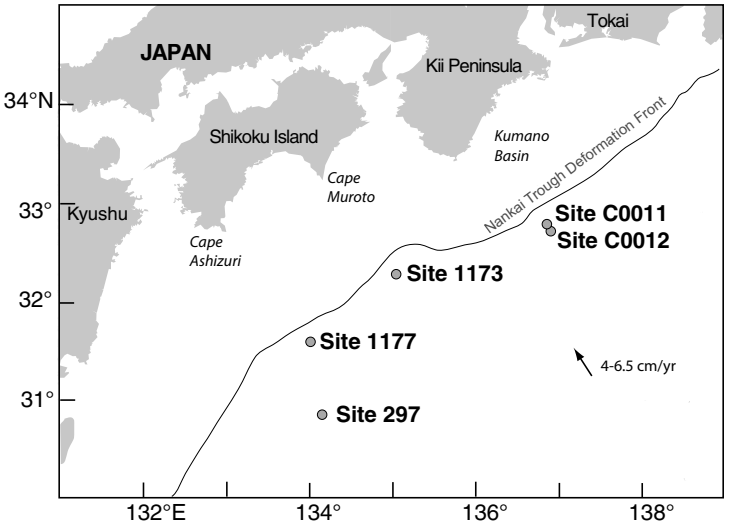

Figure 1. Map of the Nankai Trough area, offshore Japan, showing drilling locations of Deep Sea Drilling Project Site 297, Ocean Drilling Program Sites 1173 and 1177, and Integrated Ocean Drilling Program Sites C0011 and C0012 (modified from Kimura et al., 2008).

NANKAI TROUGH, SOUTHWESTERN JAPAN

Geologic Setting

Off the coast of southwestern Japan, the Nankai Trough is formed by convergence of the Philippine Sea plate and the Amurian microplate at a rate of ~4–6.5 cm/yr (Miyazaki and Heki, 2001; Loveless and Meade, 2010). Two M_w >8 earthquakes in 1944 and 1946 (Ando, 1975; Tanioka and Satake, 2001; Kikuchi et al., 2003) have made this region a key target for scientific drilling by Deep Sea Drilling Project (DSDP), Ocean Drilling Program (ODP), and Integrated Ocean Drilling Program (IODP) expeditions. Seaward of the trench, several boreholes have penetrated the input section covering >300 km along strike (Fig. 1). These sites are part of three northwest-southeast–trending borehole transects aligned with Cape Ashizuri and Cape Muroto and through the Kumano Basin. These transects show significant along-strike variations in the accretionary prism taper angle (décollement dip plus surface slope), which is on average narrower along the Muroto transect (~2°–9°) compared to the Ashizuri and Kumano transects (~5°–8° and ~6°–16°, respectively) (Taira et al., 1992; Moore et al., 2001, 2009; Kimura et al., 2007). Seafloor surface heat flow also varies along strike; high values were measured near the Muroto transect (up to ~200 mW/m^2) compared to the Ashizuri (~100–130 mW/m^2) and Kumano transects (90–140 mW/m^2) (Yamano et al., 1992, 2003; Kinoshita et al., 2008; Harris et al., 2013a).

Lithologically, several major units can be correlated across the entire margin. These include (sequentially with increasing depth) an upper unit of hemipelagic mudstone with abundant volcanic ash, monotonic hemipelagic mudstone, hemipelagic mudstone containing coarser turbidites, and a lower unit characterized by volcaniclastic material (Figs. 2–6). These units are recognized at all five Nankai Trough input sites studied here: Sites 297 (DSDP Leg 31; Shipboard Scientific Party, 1975) and 1177 (ODP Leg 190; Shipboard Scientific Party, 2001a) on the Ashizuri transect; Site 1173 (ODP Leg 190; Shipboard Scientific Party, 2001b) on the Muroto transect; and Sites C0011 and C0012 (IODP Expeditions 322 and 333; Saito et al., 2010; Henry et al., 2012) on the Kumano transect. During the Leg 190 expedition, the upper ash-rich mudstone was named the upper Shikoku Basin (USB) facies, and the underlying mudstone and mudstone with turbidites was named the lower Shikoku Basin (LSB) facies. In the two Kumano transect sites, an additional unit of volcanic turbidites was observed between the USB and LSB facies and thus named the middle Shikoku Basin (MSB) facies. Other locally observed units include red pelagic clay at the base of Site C0012, a turbiditic trench wedge facies at the top of Site 1173, and clay-rich nannofossil ooze between the USB- and LSB-equivalent units at Site 297. Basaltic basement was reached in each transect, at Sites 1177, 1173, and C0012.

Friction of Nankai Trough Inputs

Laboratory friction experiments were conducted in a modified Wykeham-Farrance rotary shear device for remolded samples from Ashizuri transect Sites 297 and 1177 (Brown et al., 2003; Kopf, 2013) at ≤2 MPa effective normal stress (assuming no excess pore pressure) and a shear rate of 1.5 µm/s. We report the coefficient of sliding friction as the ratio of measured shear stress to effective normal stress. For this study, we include the results of experiments on samples from Muroto Site 1173 following this same procedure. Downhole profiles of frictional strength measurements were conducted on intact samples from Sites C0011 and C0012 at in situ effective normal stresses (≤5 MPa) and 10 µm/s shearing velocity in a single-direct shear apparatus by Ikari et al. (2013a). Intact samples preserve in situ effects such as fabric or cementation; however, for other boreholes in the Nankai Trough, some studies have found that these effects on friction are small (Ikari and Saffer, 2011; Saffer et al., 2012). The Nankai data set is supplemented by triaxial experiments on an intact sample of LSB mudstone from Site 1173 (Bourlange et al., 2004) and intact samples from the ash-rich USB facies at Sites C0011 and C0012 (Stipp et al., 2013). We note that the values from Stipp et al. (2013) are reported as a coefficient of internal friction.

Residual friction coefficient values in samples of input material to the Nankai Trough range from as low as µ = 0.11 to as high as µ = 0.72 (Figs. 2–6; Table 1). In general, low friction (µ ≤ ~0.2) is commonly observed in the hemipelagic LSB facies while higher friction values (µ ≥ ~0.5) commonly occur in lithologic units containing volcanic material and/or turbidites. This pattern is observed margin-wide at all sites in this study. In some cases, samples within

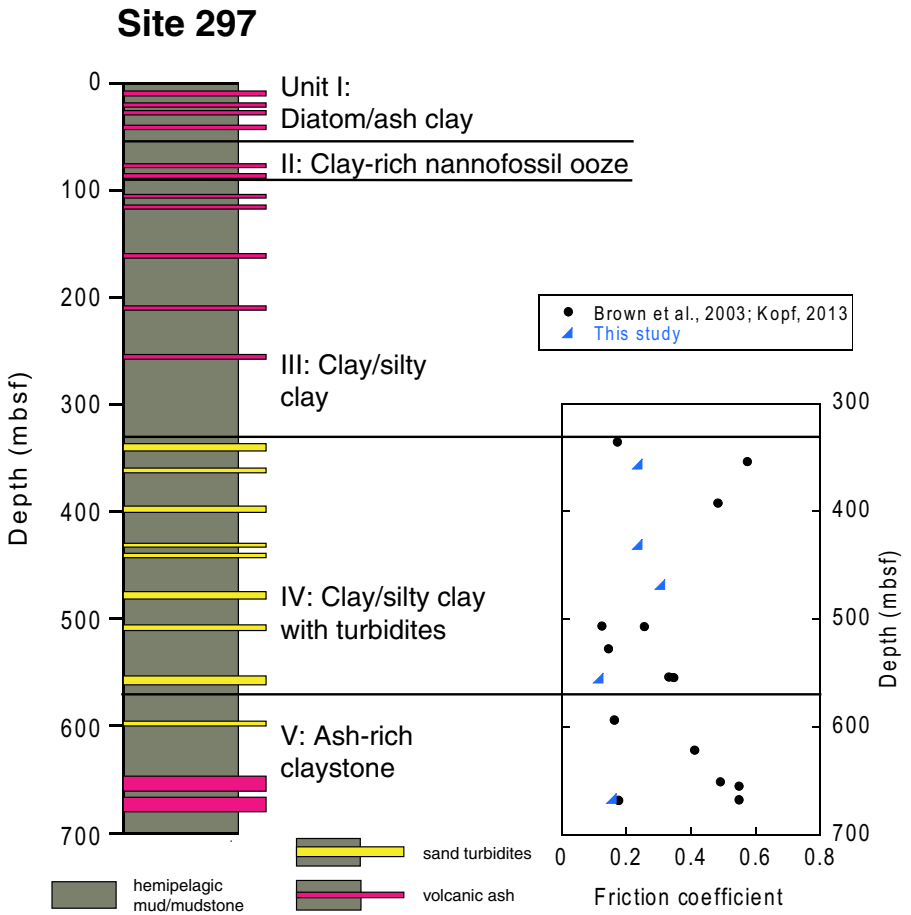

Figure 2. Lithology and experimental friction results for Deep Sea Drilling Project Site 297 at the Nankai Trough, offshore Japan (lithostratigraphy from Pickering et al., 1993). See Figure 1 for location. mbsf—meters below seafloor.

an individual lithologic unit may exhibit a wide range of friction values. Examples include the turbidite-bearing clay and silty clay and the ash-rich claystone from the Site 297 borehole (μ = 0.12–0.58); another is the volcanic turbidite (MSB) facies at Site C0012 (μ = 0.19–0.72).

JAPAN TRENCH, NORTHEASTERN JAPAN

Geologic Setting

At the Japan Trench, northeast of the Nankai Trough, the Pacific plate subducts beneath the North American–Okhotsk plate at a rate of ~8.3 cm/yr (DeMets et al., 2010). In the wake of the 2011 M_w 9 Tohoku-Oki earthquake, scientific drilling was carried out in the Japan Trench subduction zone ~1 yr later. Determining why such a large amount of coseismic slip was able to occur at extraordinarily shallow depths was one major goal of IODP Expedition 343, the Japan Trench Fast Drilling Project (JFAST) (Chester et al., 2013a). During JFAST, coring and sampling was carried out in the toe of the Japan Trench subduction zone at Site C0019, located ~7 km landward from the trench axis (Fig. 7). A corresponding input site was not drilled during JFAST, however Site 436 was drilled during DSDP Leg 56 (Shipboard Scientific Party, 1980) and is located ~250 km north-northeast of Site C0019, seaward of the Japan Trench (Fig. 7).

Core sampling at Site C0019 was concentrated within ~650–840 m below seafloor (mbsf). The prism material is dominated by relatively structureless,

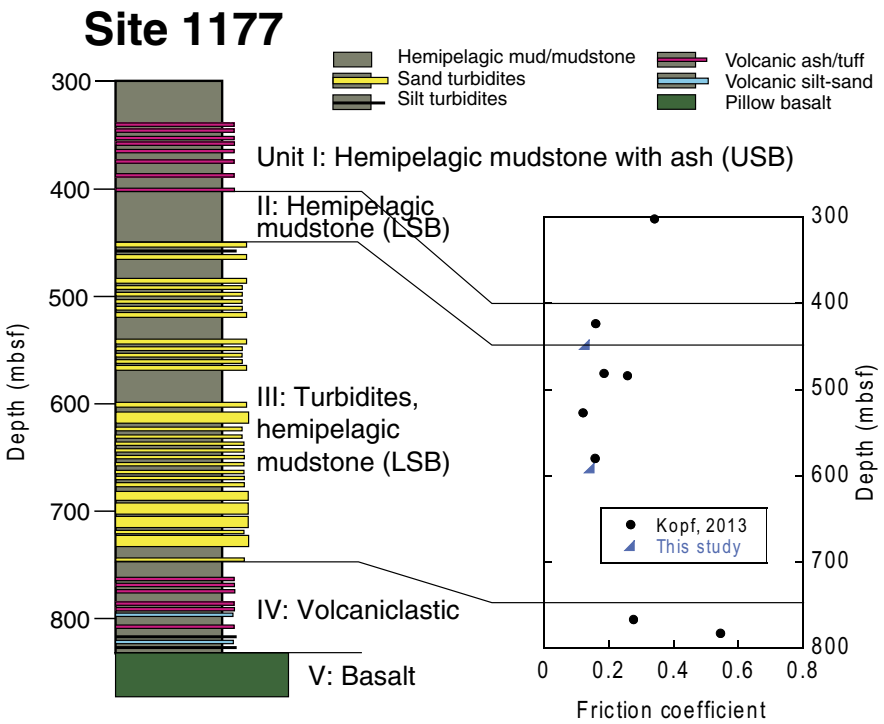

Figure 3. Lithology and experimental friction results for Ocean Drilling Program Site 1177 at the Nankai Trough, offshore Japan (lithostratigraphy from Shipboard Scientific Party, 2001a). See Figure 1 for location. mbsf—meters below seafloor; USB—upper Shikoku Basin facies; LSB—lower Shikoku Basin facies.

indurated dark gray mudstone. At 821.5–822.5 mbsf, a zone of scaly clay with intense deformation fabric was observed, which is interpreted to be the plate boundary fault zone (but not necessarily the principal slip zone of the Tohoku-Oki earthquake) (Chester et al., 2013b). The underthrust material consists of brown siliceous mudstone overlying layered pelagic clay overlying chert. At Site 436, four major units were identified: diatomaceous silty clay and claystone (unit I, further subdivided into IA and IB based on higher induration in IB), yellowish-brown diatomaceous claystone (unit II), pelagic clay (unit III), and chert and porcellanite (unit IV) (Shipboard Scientific Party, 1980). Thus, the three lowermost units at Site 436 correlate with the underthrust section at Site C0019 (Chester et al., 2013b; Kirkpatrick et al., 2015; Moore et al., 2015). At Site C0019, there are two clay-rich layers: the pelagic clay that correlates with unit III at Site 436, and the scaly clay that defines the plate boundary fault zone. It is suggested that the scaly clay décollement at Site C0019 is derived from the pelagic clay unit; the occurrence of the brown mudstone between these units is proposed to be the result of duplexing during subduction (Kirkpatrick et al., 2015).

Friction of Japan Trench Inputs

Limited friction data are available for samples from the input Site 436. Sawai et al. (2014) conducted rotary experiments at 0.7 and 2 MPa normal stress on two disaggregated samples: one from the unit II siliceous mudstone, and one from the unit III pelagic clay. They employed slip rates of 250 µm/s to 1.3 m/s, of which we use for comparison the data from their slowest tests, which have not experienced additional weakening due to dynamic effects at high experimental slip velocities (e.g., Di Toro et al., 2011). For this study, we conducted rotary shear tests on four samples representing each unit at Site 436, which follow the methodology described by Brown et al. (2003) and Kopf (2013). This data set is supplemented by a downhole profile of friction measurements using samples from the JFAST borehole Site C0019, which is in the prism landward of the deformation front. Residual friction coefficients for both intact and disaggregated Site C0019 samples were measured in a single-direct shear apparatus under in situ effective stresses (5–7 MPa) and at a shearing rate of 10 µm/s (Ikari, 2015; Ikari et al., 2015).

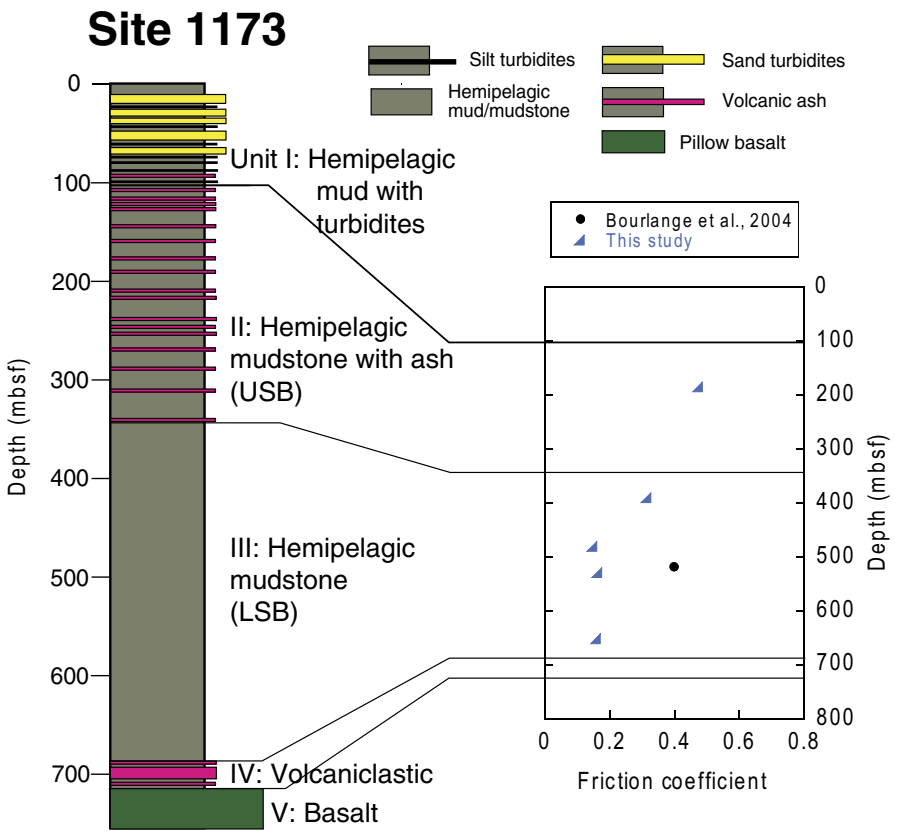

Figure 4. Lithology and experimental friction results for Ocean Drilling Program Site 1173 at the Nankai Trough, offshore Japan (lithostratigraphy from Shipboard Scientific Party, 2001b). See Figure 1 for location. mbsf—meters below seafloor. USB—upper Shikoku Basin facies; LSB—lower Shikoku Basin facies.

At Site 436, residual friction coefficients exhibit a large decrease with depth, from μ = 0.65 in the unit IA diatomaceous silty clay to as low as μ = 0.09 in the unit III pelagic clay (Fig. 8; Table 2). We note that although the lowermost chert unit was not tested in friction experiments, shipboard measurements of unconfined compressive strength for intact Site C0019 core samples show that the chert is about an order-of-magnitude stronger than all other sediments (Chester et al., 2013a). Sawai et al. (2014) found a very large friction contrast between the pelagic clay (μ = 0.09) and the overlying brown siliceous mudstone (μ = 0.52). The rotary shear data from our study also show that the pelagic clay is weaker, but the contrast is somewhat smaller (pelagic clay μ = 0.16, mudstone μ = 0.38). For samples from the JFAST borehole at Site C0019, Ikari et al. (2015) showed that the friction coefficient of the underthrust brown mudstone exhibits a wide range from μ = 0.26 to μ = 0.54, consistent with the values reported by both Sawai et al. (2014) and this study (Fig. 8; Table 2). Very low friction coefficient values (μ = 0.16–0.26) are reported for the fault zone and pelagic clay layer from Site C0019 (Ikari et al., 2015), also consistent with the weakness of the pelagic clay at Site 436. Comparison of residual friction values between intact and remolded Site C0019 samples revealed little difference.

MIDDLE AMERICA TRENCH, COSTA RICA

Geologic Setting

At the Middle America Trench offshore Costa Rica, the Cocos plate subducts beneath the Caribbean plate at a rate of ~8.8 cm/yr (DeMets et al., 2010) (Fig. 9). In this region, two types of oceanic crust are subducting, originating from the East Pacific Rise to the north and from the Cocos-Nazca spreading center to the south (Fig. 9). The boundary between these two types of crust is an ancient fracture zone, which intersects the Middle America Trench at about

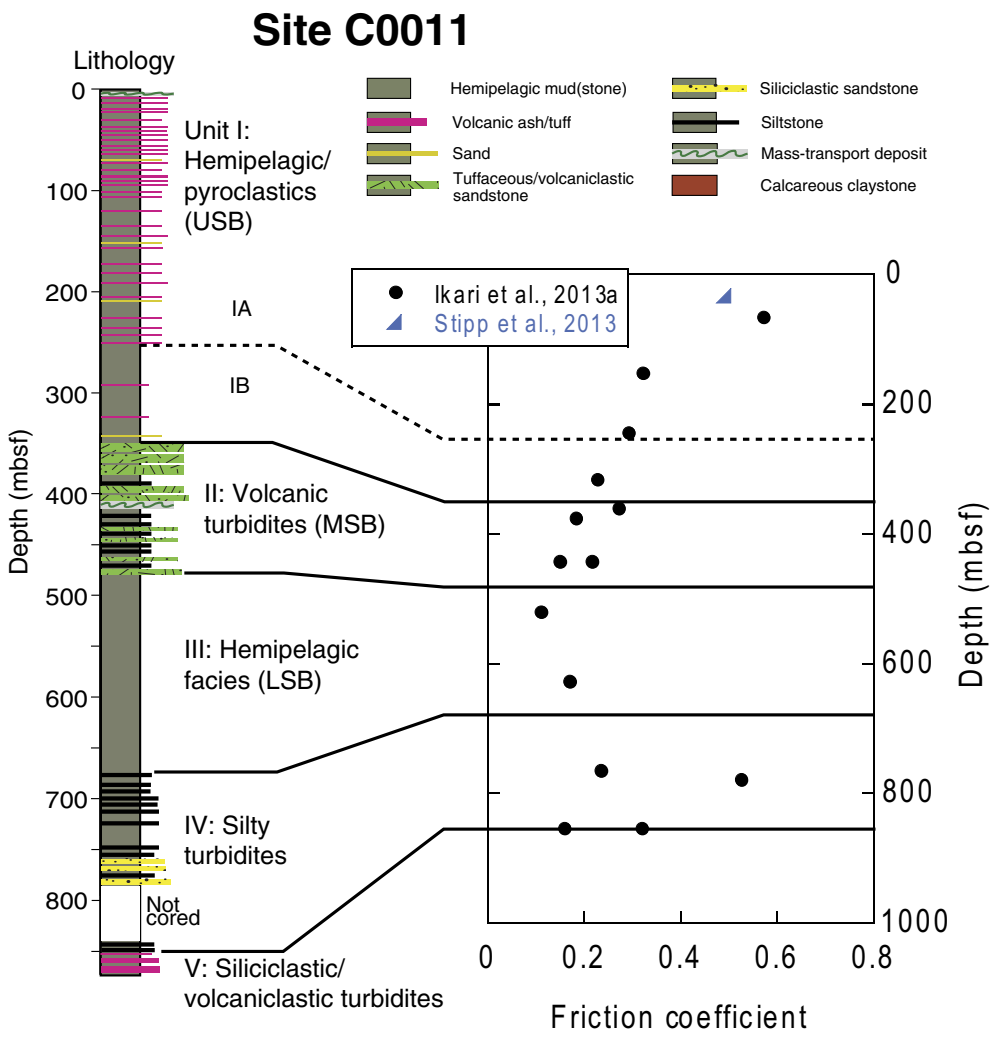

Figure 5. Lithology and experimental friction results for Integrated Ocean Drilling Program Site C0011 at the Nankai Trough, offshore Japan (lithostratigraphy from Henry et al., 2012). See Figure 1 for location. mbsf—meters below seafloor; USB—upper Shikoku Basin facies; MSB—middle Shikoku Basin facies; LSB—lower Shikoku Basin facies.

the same latitude as the southern tip of Nicoya Peninsula, Costa Rica (Hey, 1977; Barckhausen et al., 2001). There is a marked difference between the two types of crust; the East Pacific Rise crust (near-surface heat flow ≤~40 mW/m^2) is much cooler than the Cocos-Nazca spreading center crust (≥~110 mW/m^2) (Fisher et al., 2003; Harris et al., 2010a, 2010b). The East Pacific Rise crust is also bathymetrically smooth compared to the Cocos-Nazca spreading center crust, on which several 1–2.5-km-high seamounts and the 3-km-high Cocos Ridge are subducting (Hey, 1977; Ranero and von Huene, 2000; von Huene et al., 2000). These differences in topography have a major effect on sediment thicknesses and the lithology that is exposed at the seafloor (Spinelli and Underwood, 2004). The Middle America Trench is considered to be undergoing active subduction erosion at a large scale (Meschede et al., 1999; Ranero and

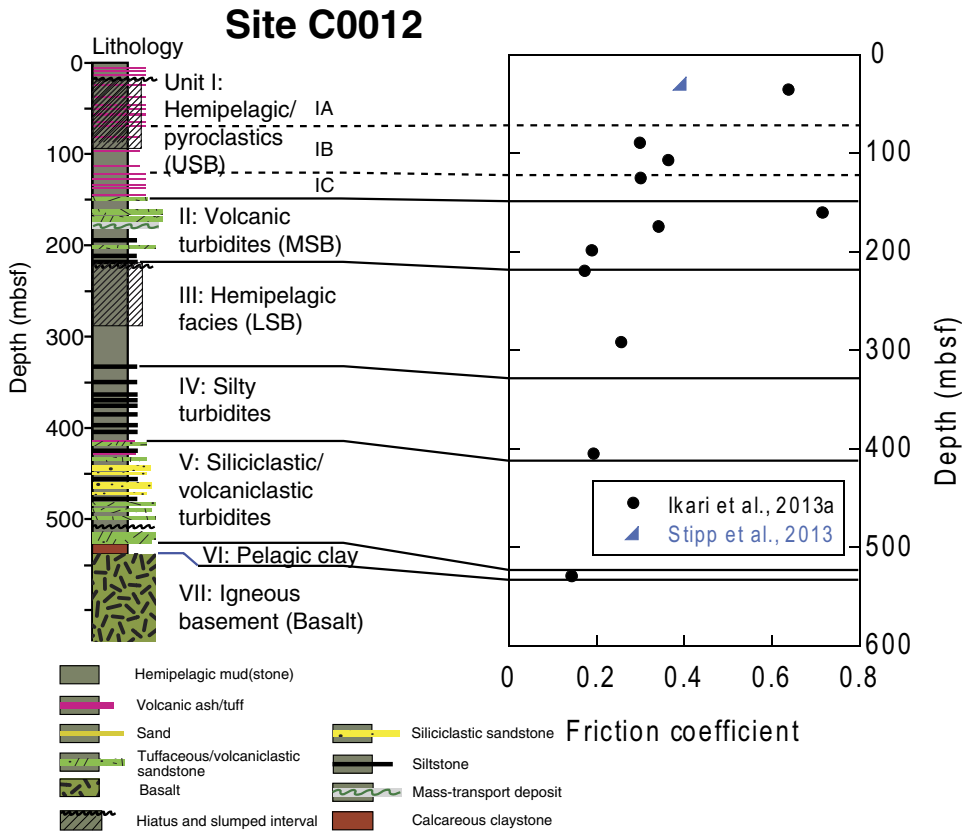

Figure 6. Lithology and experimental friction results for Integrated Ocean Drilling Program Site C0012 at the Nankai Trough, offshore Japan (lithostratigraphy from Henry et al., 2012). See Figure 1 for location. mbsf—meters below seafloor; USB—upper Shikoku Basin facies; MSB—middle Shikoku Basin facies; LSB—lower Shikoku Basin facies.

von Huene, 2000; Vannucchi et al., 2003). Nearly the entire sediment column appears to be subducting, although seismic reflection studies show evidence of a small (<10 km wide) accretionary prism near the trench with duplexing and out-of-sequence thrusting (Shipley et al., 1992; Hinz et al., 1996). The Costa Rica subduction zone has recently hosted large earthquakes of M_w 7+ (Protti et al., 1995; Husen et al., 2002; Bilek, 2007; Yue et al., 2013).

Scientific drilling at the Costa Rica margin during ODP Leg 170 (Kimura et al., 1997) and Leg 205 (Morris et al., 2003) was carried out offshore Nicoya Peninsula. In this study, we focus on two input sites drilled on the Cocos plate <2 km seaward of the deformation front: Sites 1039 (Leg 170) and 1253 (Leg 205). Site 1039, in particular, revealed ~180 m of hemipelagic siliceous ooze and claystone overlying ~220 m of siliceous ooze, calcareous ooze, and nannofossil chalk. The chalk layer was also cored and sampled at nearby Site 1253. More recent drilling has been initiated as the Costa Rica Seismogenesis Project (CRISP) during IODP Expeditions 334 (Vannucchi et al., 2012) and 344 (Harris et al., 2013b) offshore Osa Peninsula to the southeast. Two input sites have been drilled in this location: Site U1381 during Expedition 334, and Site U1414 during Expedition 344, both located ~5 km from the deformation front. Both sites show an upper layer of clay and silty clay overlying siliceous and calcareous oozes, lithologically similar to the Nicoya sites.

Friction of Costa Rica Inputs

All Costa Rica friction data for this study were obtained in rotary shear using disaggregated samples. For the input Site 1039 offshore Nicoya Peninsula, friction data were reported by Kopf (2013) for (effective) normal stresses of 4–15 MPa and slip rates of 0.01–100 µm/s. Namiki et al. (2014) sheared samples from the Osa Peninsula input Site U1381 at 5 MPa normal stress and slip rates of 2.8–280 µm/s. Studies by Ikari et al. (2013b) for Sites 1039 and 1253 and by

TABLE 1. FRICTION AND MINERAL ASSEMBLAGE DATA FOR NANKAI TROUGH DRILL SITES, OFFSHORE JAPAN

Leg / Expedition	Site	Core sample	Depth (mbsf)	(Effective) normal stress (MPa)	Slip velocity (mm/s)	Friction coefficient	Friction reference	Core sample*	Depth (mbsf)*	Total clay (%)	Smectite (in bulk sediment) (%)	XRD reference
DSDP 31	297	15-2	336.1	0.8, 1.6	1.5, 7.4	0.17	1, 2	–	–	74	19	3
DSDP 31	297	16-2	354.6	0.6	1.5	0.58	1, 2	–	–	28	5	3
DSDP 31	297	16-3	356.3	0.6	1.5, 7.4	0.24	4	–	–	21	5	3
DSDP 31	297	17-2	393.1	0.7	1.5, 7.4	0.49	1, 2	–	–	40	17	3
DSDP 31	297	18-2	430.9	0.8, 1.6	1.5, 7.4	0.24	4	–	–	63	12	3
DSDP 31	297	19-1	467.9	0.8, 1.2	0.3–7.4	0.31	4	–	–	64	19	3
DSDP 31	297	20-2	506.8	0.8–2.4	1.5, 7.4	0.13	1, 2	–	–	89	87	3
DSDP 31	297	20-2	507.1	0.8–1.6	1.5, 7.4	0.26	1, 2	–	–	64	36	3
DSDP 31	297	21-3	527.8	0.8–2.4	1.5, 7.4	0.15	1, 2	–	–	79	35	3
DSDP 31	297	22-2	554.2	0.8, 1.1	1.5, 7.4	0.33	1, 2	–	–	51	11	3
DSDP 31	297	22-2	554.4	0.8–2.2	1.5, 7.4	0.12	4					
DSDP 31	297	22-2	554.6	0.8, 1.0	1.5, 7.4	0.35	1, 2	–	–	44	30	3
DSDP 31	297	23-3	594.0	1.2–2.2	1.5	0.17	1, 2	–	–	74	49	3
DSDP 31	297	24-3	621.7	0.8	1.5	0.41	1, 2	–	–	63	38	3
DSDP 31	297	25-3	651.2	0.8	1.5	0.49	1, 2	–	–	78	50	3
DSDP 31	297	25-6	655.2	0.7	1.5	0.55	1, 2	–	–	72	51	3
DSDP 31	297	26-1	666.1	0.8–2.2	1.5, 7.4	0.16	4	–	666.3	81	53	3
DSDP 31	297	26-2	668.0	0.6	1.5, 7.4	0.55	1, 2	–	–	89	88	3
DSDP 31	297	26-2	668.6	1.6–2.3	1.5	0.18	1, 2	–	–	87	83	3
ODP 190	1177	1R2	302.6	0.9	1.5, 7.4	0.34	1	–	–	50	16	5, 6
ODP 190	1177	13R-CC	424.5	0.7	1.5–37	0.16	1	–	424.8	56	24	5, 6
ODP 190	1177	16R3	448.2	0.9	1.5, 7.4	0.13	4	–	–	55	19	5, 6
ODP 190	1177	19R-CC	482.2	0.9	1.5, 7.4	0.19	1	19R7	482	54	17	5, 6
ODP 190	1177	20R-CC	485.0	0.9	1.5, 7.4	0.26	1	20R1, 20R2	483, 484.5	49	14	5, 6
ODP 190	1177	24R5	527.7	1.1	1.5, 7.4	0.12	1	–	–	57	26	5, 6
ODP 190	1177	30R2	580.4	1.0	0.3–7.4	0.16	1	–	–	60	39	5, 6
ODP 190	1177	31R-CC	591.2	0.7, 1.0	0.3–7.4	0.15	4	–	–	61	43	5, 6
ODP 190	1177	49R5	767.8	0.7	1.5, 7.4	0.28	1	–	768.0	63	41	5, 6
ODP 190	1177	51R2	783.3	0.6	1.5, 7.4	0.55	1	–	782.3, 782.4	61	42	5, 6
ODP 190	1173	20H5	185.4	0.7, 1.0	0.3–7.4	0.48	4	20H4	184.0	39	14	7, 6
ODP 190	1173	42X2	391.2	1.0	0.3–7.4	0.32	4	–	392	58	28	7, 6
ODP 190	1173	51X5	481.3	1.0	0.3–7.4	0.15	4	–	481.5	52	30	7, 6
ODP 190	1173	55X5	520.0	3.1–3.3		*0.40*	8		520.4	60	21	7, 6
ODP 190	1173	56X5	529.6	0.9	0.3, 1.5	0.17	4	56X4	528	57	20	7, 6
ODP 190	1173	69X4	652.9	1.0	0.3–7.4	0.16	4	–	653.2	61	25	7, 6
IODP 333	C0011	2H2	33.1	0.4–1 (Pc)	1.7–150 (axial)	*0.49*	9	–	–	62		10
IODP 333	C0011	6H3	67.9	0.5	10	*0.58*	11	–	–	51		10
IODP 333	C0011	17H5	154.6	0.9	10	*0.33*	11	17H6	155.0	67		10
IODP 333	C0011	32X6	246.4	1.4	10	*0.30*	11	–	246.0	64		10
IODP 333	C0011	41X7	318.7	1.9	10	*0.23*	11	–	–	70		10
IODP 322	C0011	3R5	363.2	2.2	10	*0.28*	11	–	–	72	43	12
IODP 333	C0011	52X3	378.5	2.3	10	*0.19*	11	–	–	71		10
IODP 322	C0011	12R3	444.5	2.9	10	*0.22*	11	–	–	68	44	12
IODP 322	C0011	12R3	444.5	5.0	10	*0.15*	11	–	–	68	44	12
IODP 322	C0011	23R3	522.8	4.9	10	*0.11*	11	–	–	67	41	12
IODP 322	C0011	35R5	629.6	4.8	10	*0.17*	11	–	629.5	69	44	12
IODP 322	C0011	53R1	767.4	5.0	10	*0.24*	11	53R2	767.3	71	53	12
IODP 322	C0011	55R3	780.9	5.1	10	*0.53*	11	–	–	30	29	12
IODP 322	C0011	58R1	856.2	5.1	10	*0.32*	11	–	–	35	20	4
IODP 322	C0011	58R1	856.2	5.3	10	*0.16*	11	–	–	35	20	4
IODP 333	C0012	4H5	28.9	0.4–1 (Pc)	1.7–150 (axial)	*0.39*	9	–	–	35	2	13
IODP 333	C0012	5H2	35.7	0.2	10	*0.64*	11	–	35.7	66		14
IODP 322	C0012	5R3	90.4	0.5	10	*0.30*	11	–	90.3	62	29	12
IODP 333	C0012	13H5	107.4	0.6	10	*0.36*	11	–	106.3	66		14
IODP 322	C0012	9R6	125.9	0.6	10	*0.30*	11	–	–	62	34	12

(*continued*)

TABLE 1. FRICTION AND MINERAL ASSEMBLAGE DATA FOR NANKAI TROUGH DRILL SITES, OFFSHORE JAPAN (*continued*)

Leg / Expedition	Site	Core sample	Depth (mbsf)	(Effective) normal stress (MPa)	Slip velocity (mm/s)	Friction coefficient	Friction reference	Core sample*	Depth (mbsf)*	Total clay (%)	Smectite (in bulk sediment) (%)	XRD reference
IODP 322	C0012	13R3	161.0	0.9	10	*0.72*	11	–	–	43	39	12
IODP 333	C0012	12H3	175.1	1.0	10	*0.34*	11	–	174.6	64		14
IODP 322	C0012	17R4	199.2	1.2	10	*0.19*	11	–	–	69	51	12
IODP 322	C0012	19R4	220.0	5.3	10	*0.17*	11	–	–	74	47	12
IODP 322	C0012	27R3	292.6	2.0	10	*0.26*	11	–	–	74	61	12
IODP 322	C0012	39R1	405.8	2.9	10	*0.19*	11	–	–	72	47	12
IODP 322	C0012	52R3	530.0	5.0	10	*0.15*	11	–	–	47	1	4

Note: See Figure 1 for drill site locations. Pc—confining pressure. Friction coefficient value in italics indicates an intact sample. A dash means the sample number or depth for the XRD measurement is the same as the friction measurement. Blank cells mean no data. DSDP—Deep Sea Drilling Project; ODP—Ocean Drilling Program; IODP—Integrated Ocean Drilling Program; mbsf—meters below seafloor; XRD—X-ray diffraction.

*If >10 cm away from friction sample. A dash with a depth means the sample number is the same but the depth is different (because each sample has a depth range).

References cited: 1—Kopf, 2013; 2—Brown et al., 2003; 3—Underwood et al., 2003; 4—This study; 5—Shipboard Scientific Party, 2001b; 6—Steurer and Underwood, 2005; 7—Shipboard Scientific Party, 2001a; 8—Bourlange et al., 2004; 9—Stipp et al., 2013; 10—Expedition 333 Scientists, 2012a; 11—Ikari et al., 2013a; 12—Underwood and Guo, 2013; 13—Schumann et al., 2014; 14—Expedition 333 Scientists, 2012b.

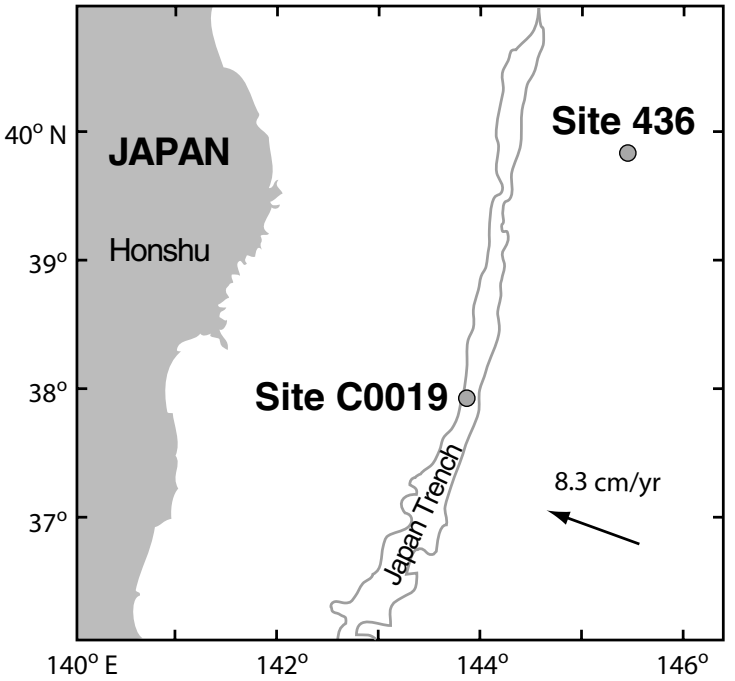

Figure 7. Map of the Japan Trench area showing drilling locations of Deep Sea Drilling Project Site 436 and Integrated Ocean Drilling Program Site C0019 (modified from Arthur and Adelseck, 1980; Kimura et al., 2008).

Kurzawski et al. (2016) for Site U1414 included a testing program that explored high pressures and temperatures, however for comparison we use their data obtained under room temperature and 15–30 MPa.

For the Nicoya input sites, the Site 1039 unit U1B diatom ooze with ash exhibits slightly lower friction coefficient values (μ = 0.28–0.34) compared to the underlying siliceous and calcareous oozes (μ = 0.40; Kopf, 2013) (Fig. 10; Table 3). The nannofossil chalk unit from Site 1253, which correlates with the base of Site 1039, was found to be very strong (μ = 0.88; Ikari et al., 2013b). A similar pattern of friction coefficient is observed in the CRISP sites offshore Osa Peninsula (Fig. 11; Table 3). Namiki et al. (2014) found that the Site U1381 unit I composed of clay and silty clay is significantly weaker (μ = 0.13–0.16) compared to the underlying siliceous and calcareous oozes (μ = 0.63–0.77). Kurzawski et al. (2016) reported the friction coefficient of the clay and silty clay of unit I at Site U1414 to be μ = 0.56; this is significantly lower than that of the calcareous nannofossil ooze of unit IIB (μ = 0.84) but higher than Namiki et al.'s (2014) values for the corresponding unit, although still lower than their values for the ooze. However, the high friction of the calcareous nannofossil ooze in the Osa Peninsula inputs matches that of the nannofossil chalk offshore Nicoya Peninsula.

IMPLICATIONS FOR SUBDUCTION ZONE PROCESSES

Lithology and Mineral Assemblage as a Control on Frictional Behavior

The shear strength of geologic materials has long been measured in laboratory deformation experiments. Many common rocks and minerals were found to have friction coefficients μ of 0.6–0.85; the strengths of quartz and calcite lie in this range (Byerlee, 1978). However, Byerlee also recognized that

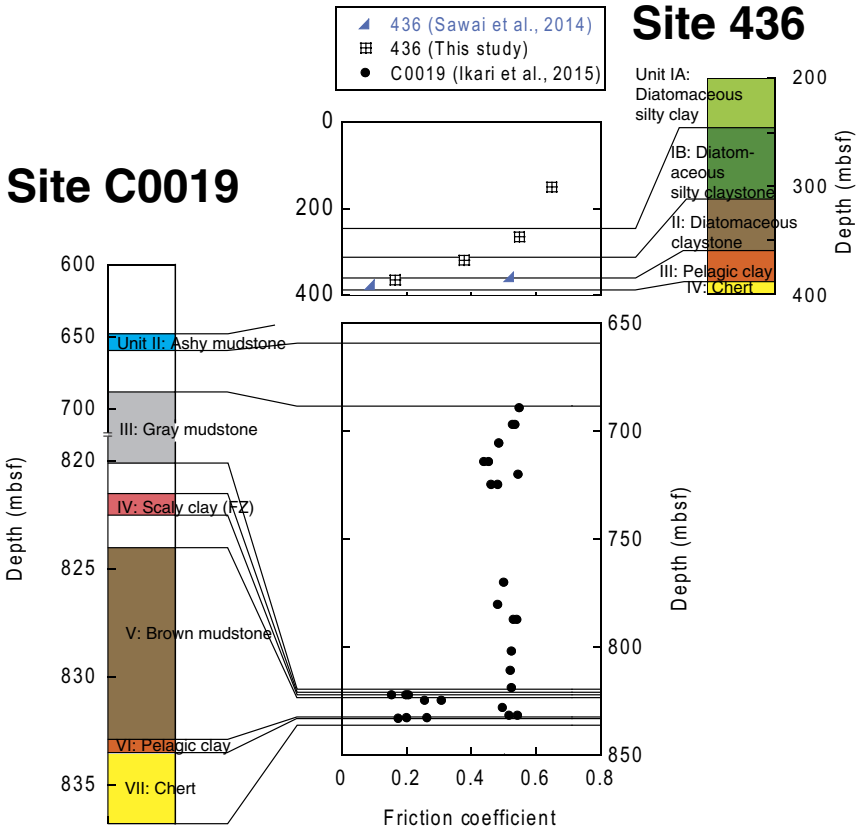

Figure 8. Lithology and experimental friction results for Deep Sea Drilling Project Site 436 and Integrated Ocean Drilling Program Site C0019 at the Japan Trench (lithostratigraphy from Shipboard Scientific Party, 1980; Chester et al., 2013a). See Figure 7 for location. Note the vertical scale change on the Site C0019 lithologic column. mbsf—meters below seafloor; FZ—fault zone.

clay minerals deviate from this range and may be significantly weaker. How much weaker depends on the mineral species, and specifically smectite was identified as the weakest material. Subsequent work has confirmed the extraordinary weakness of smectite, which may exhibit $\mu < 0.1$ in the presence of water (Lupini et al., 1981; Logan and Rauenzahn, 1987; Ikari et al., 2007; Moore and Lockner, 2007). Other common clay minerals (illite, chlorite, kaolinite) are not as weak as smectite but weaker than common framework minerals, with μ generally ranging between 0.2 and 0.4 (Morrow et al., 1992, 2000; Brown et al., 2003; Crawford et al., 2008; Ikari et al., 2009). In deep-sea sediments approaching subduction zones, certain minerals are especially relevant due to their abundance: smectite, illite, silica (quartz, volcanic ash, opal), and calcite (e.g., Rea and Ruff, 1996; Underwood, 2007).

We report mineral assemblages for our samples from X-ray diffraction (XRD) analyses. Most of these data are previously published (see Tables 1–3), supplemented by additional measurements in this study following the methods described by Vogt et al. (2002). In most cases, XRD data are available for the same samples where friction coefficients were measured. When this was not the case, we use XRD data from neighboring core samples, usually within ~1 m in depth but in some cases up to 4 m away from a sample in question.

The mineral composition of sediments approaching the Nankai Trough is highly variable. For most samples, total clay content generally ranges from ~30 to ~80 wt% and smectite abundance in the bulk sediment ranges from ~10 to ~60% (Shipboard Scientific Party, 2001a, 2001b; Underwood et al., 2003; Steurer and Underwood, 2005; Expedition 333 Scientists, 2012a, 2012b; Underwood and Guo, 2013). A wide scatter in both total clay and smectite is observed for the Ashizuri sites, but it can be seen that the Kumano sites exhibit higher total clay and higher smectite contents compared to the Muroto input Site 1173. Contrary to laboratory experiments on mineral standards, a clear negative dependence of friction on either total clay content or smectite is not visible as a result of large data scatter (Fig. 12). The scatter is also observable

TABLE 2. FRICTION AND MINERAL ASSEMBLAGE DATA FOR JAPAN TRENCH DRILL SITES

Leg / Expedition	Site	Core sample	Depth (mbsf)	(Effective) normal stress (MPa)	Slip velocity (mm/s)	Friction coefficient	Friction reference	Core sample*	Depth (mbsf)*	Total clay (%)	Smectite (in bulk sediment) (%)	XRD reference
DSDP 56	436	16R7	150.2	1.0	1.5, 7.5	0.65	This study					
DSDP 56	436	29R1	265.0	1.0	1.5, 7.5	0.55	This study					
DSDP 56	436	34R6	319.7	1.0	1.5, 7.5	0.38	This study	35R1	322.3	53	37	Kameda et al., 2015a
DSDP 56	436	38R6	358.0	0.7–2.0	250	0.52	Sawai et al., 2014	–	–	26	23	Kameda et al., 2015a
DSDP 56	436	39R4	365.0	1.0	1.5, 7.5	0.16	This study	–	364.7	82	77	Kameda et al., 2015a
DSDP 56	436	40R6	376.8	0.7–2.0	250	0.09	Sawai et al., 2014	–	376.2	85	65	Kameda et al., 2015a
IODP 343	C0019	2R1	648.4	4.9	10	0.53	Ikari et al., 2015	–	648.5	24	17	Kameda et al., 2015a
IODP 343	C0019	4R1	689.4	5.4	10	0.55	Ikari et al., 2015	–	689.2	19	9	Kameda et al., 2015a
IODP 343	C0019	5R1	697.2	5.5	10	*0.53*	Ikari et al., 2015	–	–	24	15	Kameda et al., 2015a
IODP 343	C0019	5R1	697.2	5.5	10	0.54	Ikari et al., 2015	–	–	24	15	Kameda et al., 2015a
IODP 343	C0019	6R2	705.9	5.6	10	0.49	Ikari et al., 2015	–	705.3	16	11	Kameda et al., 2015a
IODP 343	C0019	7R2	714.4	5.7	10	*0.44*	Ikari et al., 2015	–	715.3	30	20	Kameda et al., 2015a
IODP 343	C0019	7R2	714.4	5.7	10	0.46	Ikari et al., 2015	–	715.3	30	20	Kameda et al., 2015a
IODP 343	C0019	8R2	720.4	5.8	10	0.55	Ikari et al., 2015	–	721.5	24	15	Kameda et al., 2015a
IODP 343	C0019	9R1	725.0	5.9	10	*0.46*	Ikari et al., 2015	–	724.6	27	17	Kameda et al., 2015a
IODP 343	C0019	9R1	725.0	5.9	10	0.48	Ikari et al., 2015	–	724.6	27	17	Kameda et al., 2015a
IODP 343	C0019	10R1	770.2	6.5	10	0.50	Ikari et al., 2015	–	770.6	24	13	Kameda et al., 2015a
IODP 343	C0019	11RCC	780.6	6.6	10	0.48	Ikari et al., 2015					
IODP 343	C0019	12R2	787.4	6.7	10	*0.54*	Ikari et al., 2015	–	–	16	10	Kameda et al., 2015a
IODP 343	C0019	12R2	787.4	6.7	10	0.53	Ikari et al., 2015	–	–	16	10	Kameda et al., 2015a
IODP 343	C0019	13R2	802.3	6.9	10	0.53	Ikari et al., 2015					
IODP 343	C0019	14R2	811.2	7.0	10	0.52	Ikari et al., 2015	14R1	810.0	27	14	Kameda et al., 2015a
IODP 343	C0019	16R1	819.1	7.1	10	0.53	Ikari et al., 2015	–	818.6	25	14	Kameda et al., 2015a
IODP 343	C0019	17R1	822.6	7.2	10	0.21	Ikari et al., 2015	–	–	90	70	Kameda et al., 2015a
IODP 343	C0019	17R1	822.6	7.2	10	*0.20*	Ikari et al., 2015	–	–	90	70	Kameda et al., 2015a
IODP 343	C0019	17R1	822.6	7.2	10	0.16	Ikari et al., 2015	–	–	90	70	Kameda et al., 2015a
IODP 343	C0019	18R1	824.9	7.2	10	0.31	Ikari et al., 2015	–	–	49	34	Kameda et al., 2015a
IODP 343	C0019	18R1	824.9	7.2	10	0.26	Ikari et al., 2015	–	–	49	34	Kameda et al., 2015a
IODP 343	C0019	19R2	828.4	7.3	10	0.50	Ikari et al., 2015	–	828.1	36	21	Kameda et al., 2015a
IODP 343	C0019	20R1	831.9	7.3	10	*0.54*	Ikari et al., 2015	–	–	30	20	Kameda et al., 2015a
IODP 343	C0019	20R1	831.9	7.3	10	0.52	Ikari et al., 2015	–	–	30	20	Kameda et al., 2015a
IODP 343	C0019	20R2	833.0	7.3	10	0.26	Ikari et al., 2015	–	–	65	62	Kameda et al., 2015a
IODP 343	C0019	20R2	833.1	7.3	10	0.20	Ikari et al., 2015	–	–	30	29	Kameda et al., 2015a
IODP 343	C0019	20R2	833.3	7.3	10	0.18	Ikari et al., 2015	–	–	66	65	Kameda et al., 2015a

Note: See Figure 7 for drill site locations. Friction coefficient value in italics indicates an intact sample. A dash means the sample number for the XRD measurement is the same as the friction measurement. Blank cells mean no data. DSDP—Deep Sea Drilling Project; IODP—Integrated Ocean Drilling Program; mbsf—meters below seafloor; XRD—X-ray diffraction.

*Depth given if >10 cm away from friction sample. A dash with a depth means the sample number is the same but the depth is different (because each sample has a depth range).

when considering individual sites and transects. One possible reason for the large scatter is the presence of amorphous material such as volcanic ash and biogenic silica, which are usually not explicitly quantified in XRD analyses (e.g., Brown et al., 2003; Underwood et al., 2003).

In the Japan Trench, sediment strength is clearly controlled to first order by clay minerals, specifically smectite (Fig. 13). XRD analyses performed by Kameda et al. (2015a) on samples from Site 436 show that mineral abundances change dramatically across the boundary between the unit II diatomaceous claystone and unit III pelagic clay. At this depth (360 mbsf), total clay in the bulk sediment increases from ~30% to 60%, and smectite content in the bulk sediment increases from ~30% to as high as 80%. This pattern is also seen at Site C0019, where clearly higher total clay (up to 90%) and smectite (up to 80% of the bulk sediment) are observed in the plate boundary fault zone, and to a lesser extent in the narrow zone of pelagic clay, compared to the mudstone units (~25%–30% total clay, ~15%–20% smectite in the bulk sediment) (Kameda et al., 2015a).

For the Costa Rica input sites, mineralogic content also plays a first-order role in controlling friction. Based on available XRD data (Ikari et al., 2013b;

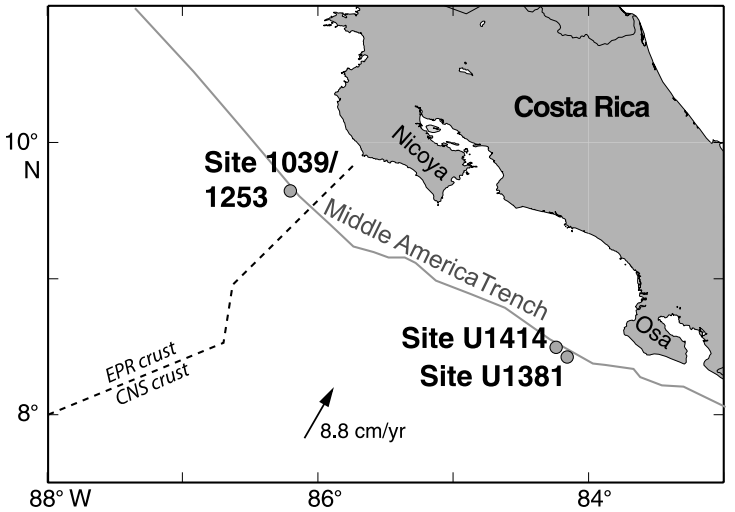

Figure 9. Map of the Middle America Trench area, offshore Costa Rica, showing drilling locations of Ocean Drilling Program Sites 1039 and 1253 Integrated Ocean Drilling Program Sites U1381 and U1414 (modified from Morris et al., 2003). EPR—East Pacific Rise; CNS—Cocos-Nazca spreading center.

Kameda et al., 2015b; Kurzawski et al., 2016), friction correlates inversely with total clay content as expected. However, smectite contents are low, no higher than 22% of the bulk sediment in the samples analyzed for this study. Due to the presence of carbonate-rich pelagic ooze and chalk, calcite may play an important role. However, calcite content exhibits a much wider range compared to total clay and only weakly correlates with friction (Fig. 14). Some samples from Costa Rica exhibit both high friction and low calcite content of <20%; these samples likely contain a significant amount of amorphous silica (Spinelli and Underwood, 2004; Kameda et al., 2015b). In general, the lithologic contrast between the hemipelagic sediments and the underlying oozes and chalks observed offshore both Nicoya and Osa Peninsulas are also associated with a significant strength contrast (Fig. 14).

Frictional Strength Variations as a Control on Subduction Zone Processes

Strongly contrasting lithologic units can be used to explain mechanical behavior in the Japan Trench. High smectite content of the pelagic clay–derived fault zone results in extreme weakness in a localized zone, which contrasts with much stronger siliceous mudstone wall rocks. This is an attractive explanation as to why the shallow décollement allowed tens of meters of coseismic slip to propagate up to the seafloor during the 2011 Tohoku-Oki earthquake (Chester et al., 2013b; Fulton et al., 2013; Ujiie et al., 2013; Ikari et al., 2015; Remitti et al., 2015). The depth extent to which the smectite-rich layer exerts control on deformation at the Japan Trench is uncertain, but subduction erosion is proposed to be occurring at greater depth (von Huene and Culotta, 1989; von Huene and Lallemand, 1990), which suggests that the influence of this layer may be limited to the near-trench region.

Another subduction zone in which smectite is considered influential is the Barbados subduction zone. There, smectite contents of up to ~50% in the bulk sediment have been measured in core samples from ODP Site 948 in the prism toe, which noticeably decrease at the base of the décollement (Deng and Underwood, 2001). It was thus proposed that smectite content influences the location and development of the décollement at Barbados.

In Costa Rica, there is a large strength contrast between the weaker hemipelagic clays found at the top of the incoming sediment column and the stronger calcareous and siliceous oozes deeper in the section. Kopf (2013) suggested that this is why the décollement initiates in the uppermost unit of the sediment inputs, which is consistent with offscraping within the hemipelagic sediment to form a small accretionary prism (Shipley et al., 1992; Hinz et al., 1996). However, any accretion is limited to within ~10 km from the deformation front, so that the Costa Rica margin is characterized by subduction erosion at a larger scale (Meschede et al., 1999; Ranero and von Huene, 2000; Vannucchi et al., 2003). Von Huene et al. (2000) used seismic reflection and bathymetry data to conclude that subduction erosion is most pronounced where topographic highs such as the Cocos Ridge and surrounding seamounts are subducting. Observations from a shallow coring campaign offshore Nicoya Peninsula revealed that on bathymetric highs, the hemipelagic cover is either severely reduced or absent, leaving the carbonate-rich ooze or chalk exposed at the seafloor (Spinelli and Underwood, 2004). Therefore, we speculate that at greater depth beyond the small accretionary prism, the much higher friction of the ooze and chalk shearing against the upper plate may be one reason for the development of subduction erosion, supporting the conclusions of von Huene et al. (2000). Additionally, Ikari et al. (2013b) suggested that the frictional properties of the carbonate-rich pelagic sediment are favorable for seismogenic behavior, and that topographically controlled occurrence of shallow carbonates is consistent with observed seismicity patterns in the Nicoya area.

In the Nankai Trough, however, sharp contrasts in friction reflecting contrasts in mineral assemblage are not seen in the input sediments (Fig. 12). Correspondingly, margin-wide variations in mechanical behavior cannot be unambiguously attributed to variations in the mineral composition of the incoming sediments. For example, the décollement localizes in the clay-rich (turbidite-poor) LSB facies on both the Ashizuri and Muroto transects (Moore et al., 2001) despite the observation that smectite content is higher at the Ashizuri sites. Kopf (2013) showed that very low friction coefficients ($\mu < \sim 0.2$) tend to be observed in the LSB sediments, which explains the localization of the décollement in this unit. However, these low friction values cannot be entirely

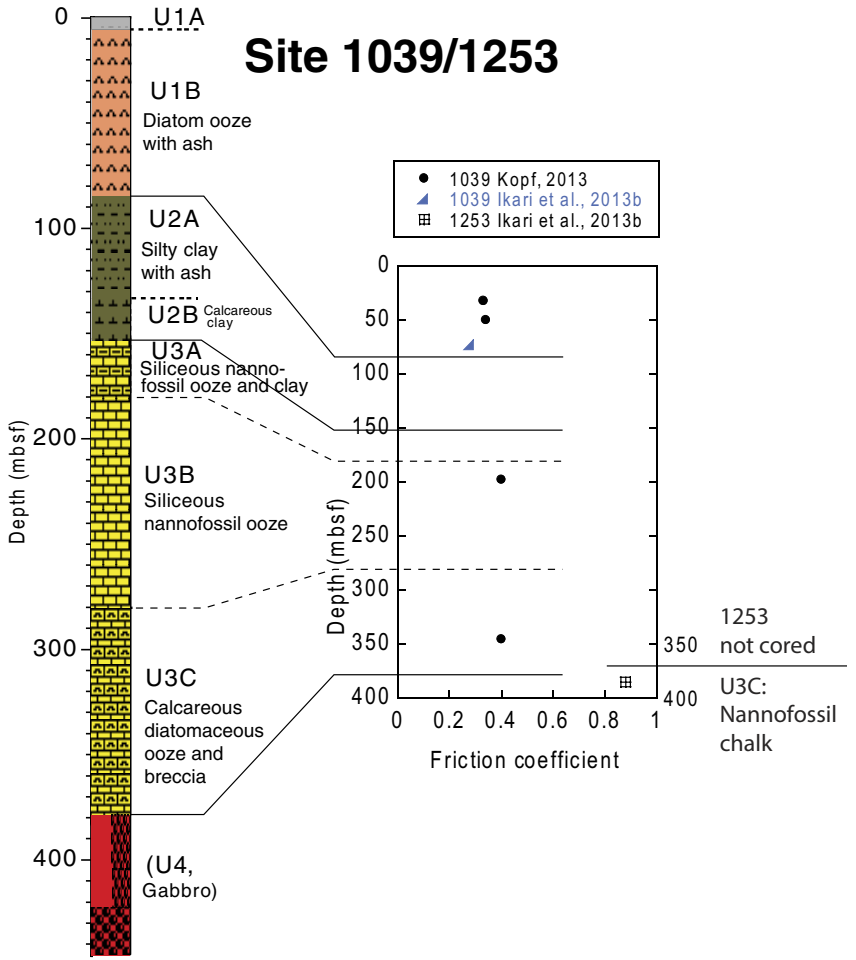

Figure 10. Lithology and experimental friction results for Ocean Drilling Program Sites 1039 and 1253 at the Middle America Trench, offshore Nicoya Peninsula, Costa Rica (lithostratigraphy from Kimura et al., 1997). See Figure 9 for location. mbsf—meters below seafloor.

explained by mineral assemblage; total clay content is generally high (50%–80%) in the weak samples from all three transects, but the smectite content is not necessarily high, and at Site 1173 is <~30%. Smectite contents on the Kumano transect are comparable with those of the Ashizuri sites, however a Coulomb wedge analysis considering the relatively steep taper angle at the toe suggests that the plate boundary occurs in the stronger, ash-bearing USB facies (Ikari et al., 2013a).

Because prism taper angles are largely controlled by the frictional strength of the décollement, they may also be expected to correlate inversely with total clay or smectite content (i.e., high clay and/or smectite should produce narrow wedge taper). The taper angle of the wedge at the Kumano transect is ~6°–16°; it is ~5°–8° at the Ashizuri transect and ~2°–9° at the Muroto transect (Taira et al., 1992; Moore et al., 2001; Kimura et al., 2007; Moore et al., 2009). Clearly, the narrow taper angle at the Muroto transect cannot be explained by elevated smectite, which is more abundant at the Ashizuri and Kumano transects. Total clay content also does not explain the differences because of the large scatter and similar range of total clay observed at all three transects. This indicates that mechanical behavior in the Nankai Trough cannot easily be explained by mineral assemblage alone, and that other processes affecting sediment strength play an important role.

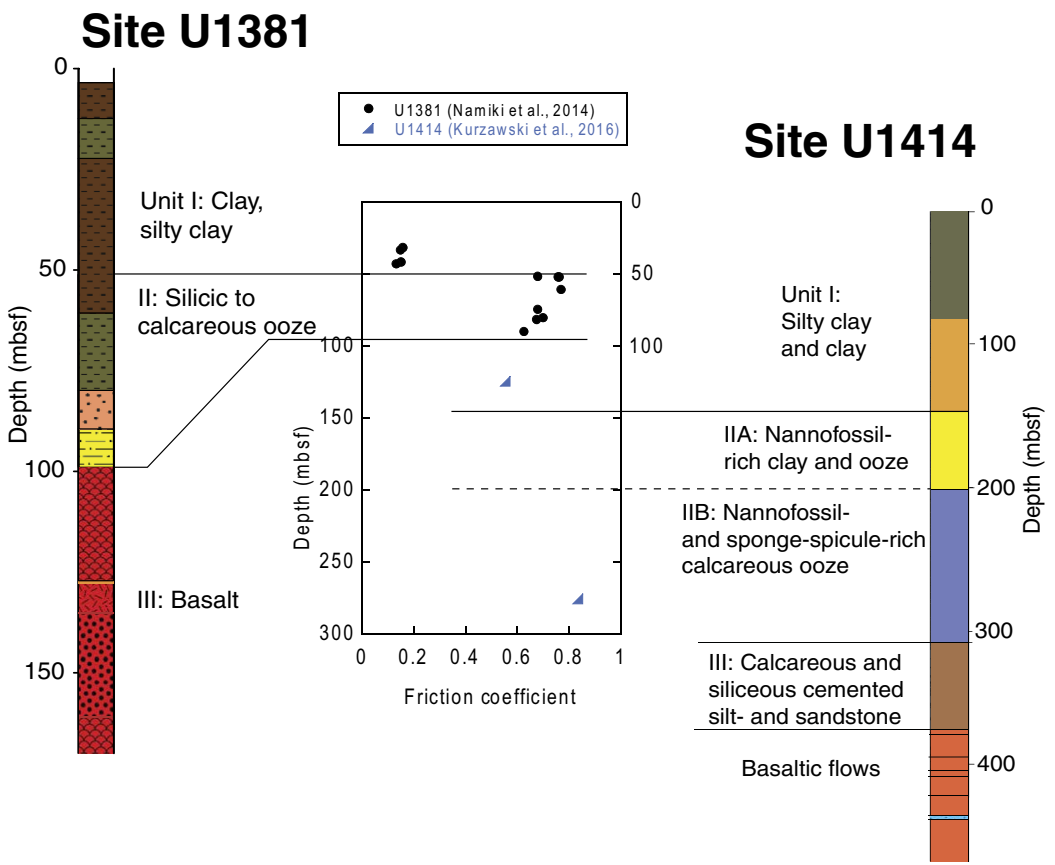

Figure 11. Lithology and experimental friction results for Integrated Ocean Drilling Program Sites U1381 and U1414 at the Middle America Trench, offshore Osa Peninsula, Costa Rica (lithostratigraphy from Vannucchi et al., 2012; Harris et al., 2013b). See Figure 9 for location. mbsf—meters below seafloor.

Secondary Effects of Composition on Sediment Strength

Diagenetic Effects

Other than mineral assemblage, a variety of other factors are known to have a significant influence on strength. Of particular relevance to sediment packages approaching subduction zones are effects of sediment diagenesis and hydrologic effects, both of which are controlled to first order by the composition of the originally deposited sediment. In many cases these effects are strongly coupled. These may be particularly important in the Nankai Trough, where lithologic differences are not associated with large contrasts in friction.

Sediment diagenesis can cause drastic changes in the bulk sediment composition, with the alteration of volcanic ash to authigenic smectite being particularly relevant to this study. The transformation is a function of increasing temperature and time, and thus the extent of the reaction increases with burial depth (e.g., Vrolijk, 1990; Hodder et al., 1993; Masuda et al., 1996). Direct shear experiments on mixtures of tephra and smectite show that friction coefficients range from μ = ~0.85 for pure tephra to μ = ~0.17 for smectite (Wiemer and Kopf, 2015). Thus, sediment friction may be expected to decrease drastically with depth as the reaction progresses; this would help explain the general downhole trend of decreasing friction observed in the Nankai Trough input sediments. With further burial, smectite transforms to illite; this reaction is most active at temperatures of 60–100 °C and approaches completion by 150 °C (Pytte and Reynolds, 1989). Of the sites considered in this study, temperatures are high enough for nearly full conversion of smectite to illite only in the basal sediment of Site 1173, as inferred from anomalously high surface heat flow on the Muroto transect (Saffer et al., 2008). Illite is stronger than smectite (Morrow et al., 1992; Brown et al., 2003; Ikari

TABLE 3. FRICTION AND MINERAL ASSEMBLAGE DATA FOR MIDDLE AMERICA TRENCH DRILL SITES, OFFSHORE COSTA RICA

Leg / Expedition	Site	Core sample	Depth (mbsf)	(Effective) normal stress (MPa)	Slip velocity (mm/s)	Friction coefficient	Friction reference	Core sample*	Depth (mbsf)*	Total clay (%)	Smectite (in bulk sediment) (%)	Calcite (%)	XRD reference
ODP 170	1039	5H2	32.2	4–15	0.01–100	0.33	Kopf, 2013	-	-	63	14	0	This study
ODP 170	1039	7H1	49.8	4–15	0.01–100	0.34	Kopf, 2013	6H4	45.8	50	17	0	This study
ODP 170	1039	9H3	72.9	30	10	0.28	Ikari et al., 2013b	-	-	51	22	1	Ikari et al., 2013b
ODP 170	1039	22X6	197.9	4–15	0.01–100	0.40	Kopf, 2013	22X5	197.2	0	0	96	This study
ODP 170	1039	38X2	345.6	4–15	0.01–100	0.40	Kopf, 2013	38X3	348.3	0	0	90	This study
ODP 205	1253	3R	385.2	15	10	0.88	Ikari et al., 2013b	-	-	8	3	66	Ikari et al., 2013b
IODP 334	U1381	5R1	32.2	5	280	0.16	Namiki et al., 2014	-	-	41	11	9	Namiki et al., 2014; this study
IODP 334	U1381	5R2	33.7	5	280	0.15	Namiki et al., 2014	-	-	47	7	1	Namiki et al., 2014; this study
IODP 334	U1381	6R1	42.0	5	280	0.15	Namiki et al., 2014	-	-	25	8	24	Namiki et al., 2014; this study
IODP 334	U1381	6R2	43.5	5	280	0.13	Namiki et al., 2014	-	-	32	5	29	Namiki et al., 2014; this study
IODP 334	U1381	7R1	52.2	5	280	0.68	Namiki et al., 2014	-	-	20	16	0	Namiki et al., 2014; this study
IODP 334	U1381	7R2 (black)	52.4	5	280	0.76	Namiki et al., 2014	-	-	14	14	0	Namiki et al., 2014; this study
IODP 334	U1381	7R2 (white)	52.4	5	280	0.76	Namiki et al., 2014	-	-	3	2	50	Namiki et al., 2014; this study
IODP 334	U1381	8R1	61.5	5	280	0.77	Namiki et al., 2014	-	-	1	0	60	Namiki et al., 2014; this study
IODP 334	U1381	9R4	75.0	5	280	0.68	Namiki et al., 2014	-	-	0	0	76	Namiki et al., 2014; this study
IODP 334	U1381	10R1	81.0	5	280	0.70	Namiki et al., 2014	-	-	2	1	58	Namiki et al., 2014; this study
IODP 334	U1381	10R2	82.0	5	280	0.68	Namiki et al., 2014	-	-	2	0	51	Namiki et al., 2014; this study
IODP 334	U1381	11R1	90.5	5	280	0.63	Namiki et al., 2014	-	-	0	0	72	Namiki et al., 2014; this study
IODP 344	U1414	14H6	124.7	30	10	0.56	Kurzawski et al., 2016	-	-			20	Kurzawski et al., 2016
IODP 344	U1414	30X7	276.0	30	10	0.84	Kurzawski et al., 2016	-	-			89	Kurzawski et al., 2016

Note: See Figure 9 for drill site locations. A dash means the sample number for the XRD measurement is the same as the friction measurement. Blank cells mean no data. ODP—Ocean Drilling Program; IODP—Integrated Ocean Drilling Program; mbsf—meters below seafloor; XRD—X-ray diffraction.

*Depth given if >10 cm away from friction sample. A dash with a depth means the sample number is the same but the depth is different (because each sample has a depth range).

et al., 2009), so friction coefficients might be expected to increase deeper in the Muroto transect boreholes. However, there is no evidence of such a pattern in our data for Site 1173 (Fig. 4). Furthermore, Saffer et al. (2012) sheared intact mudstones recovered from the nearby Site 1174 located across the trench in the accretionary prism toe on the Muroto transect, where high heat flow is hypothesized to drive advanced diagenesis. They observed that the measured frictional properties are independent of both in situ temperature and smectite-illite reaction progress, and therefore concluded that diagenesis in this area has not progressed enough to affect sediment mechanical behavior.

An aspect of diagenesis that may significantly affect strength is cementation. Both the ash-to-smectite and smectite-to-illite reactions release silica into the pore water, which may precipitate and function as cement (Towe, 1962; Singer and Müller, 1979; Kastner et al., 2014). In the ash-rich USB facies, for example, high silica concentrations of up to 800–1000 μM in pore waters facilitated precipitation of amorphous silica. This effect has led to the formation of a Nankai margin-wide zone of anomalously high porosity, which was suggested to be caused by diagenetic cementation (e.g., Spinelli et al., 2007; Raimbourg et al., 2011; White et al., 2011). However, low measured values of cohesion in intact samples from Sites C0011 and C0012 indicate a lack of cementation (Ikari et al., 2013a). It has been therefore suggested that the origin of the high-porosity zone is not cementation of the bulk sediment, but rather the formation of locally confined aggregates from patchy precipitation of amorphous silica (Hüpers et al., 2015).

In contrast to the Nankai Trough, silica cementation is likely advanced in the Japan Trench. An intact sample of the siliceous mudstone from between the décollement and pelagic clay at Site C0019, which correlates with the diatomaceous claystone at Site 436, exhibited a cohesion value of 220 kPa (Ikari et al., 2015). In comparison, measured cohesion of mudstones from Sites C0011 and C0012 along the Kumano transect at the Nankai Trough ranges from 13 to 160 kPa (Ikari et al., 2013a), consistent with calculated cohesion values of 35 and 41 kPa for two samples from these sites (Stipp et al., 2013). There is a large amount of amorphous silica in the Japan Trench mudstone unit, up to ~60% at both Sites C0019 and 436 (Kameda et al., 2015a), which might indicate advanced cementation. Furthermore, diagenesis in the Japan Trench has advanced so that chert and porcellanite is observed at the bottom of both boreholes. For the Costa Rica subduction zone, cementation was used to explain low instances of compression index (i.e., high stiffness) in the carbonate unit (Saffer, 2003). In the case of both the Japan Trench and Costa Rica, we speculate that diagenetic cementation effects likely enhance the strength of clay-poor lithologies, and possibly also the strength contrast between high-clay and high-smectite layers and the more siliceous and carbonate-rich units.

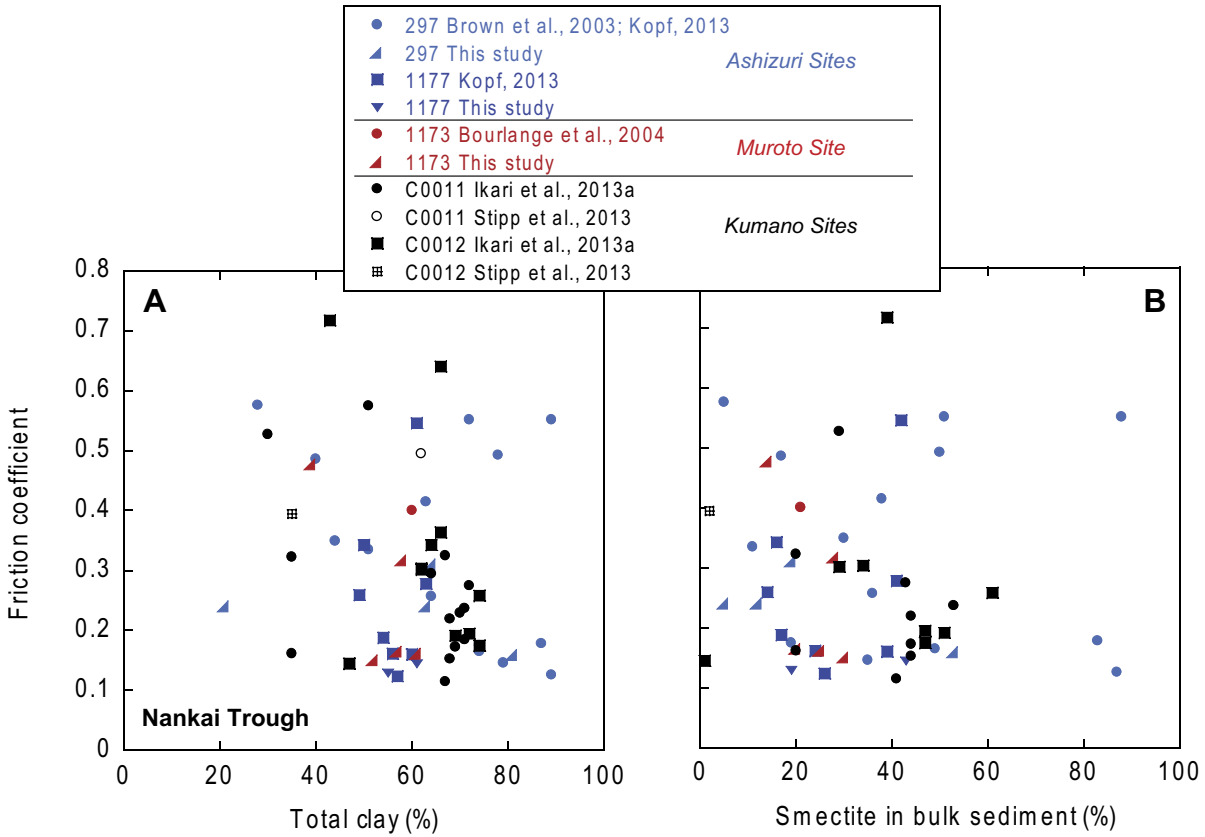

Figure 12. Friction coefficient as a function of total clay minerals (A) and smectite content in the bulk sediment (B) for the Nankai Trough drilling sites, offshore Japan (see Fig. 1 for locations). Mineral content data are from Shipboard Scientific Party (2001a, 2001b), Underwood et al. (2003), Steurer and Underwood (2005), Expedition 333 Scientists (2012a, 2012b), and Underwood and Guo (2013). Note that for some samples, smectite content is not available (see Table 1).

Hydrologic Effects

The strength of sediments is also strongly controlled by hydrologic effects, specifically the development of excess pore pressure. Elevated pore pressures lower the effective normal (or vertical, in the case of input sediments) stress and thus lower the shear stress necessary for failure, without necessarily changing the friction coefficient. Although full discussion of elevated pore pressure causes and distribution is beyond the scope of this work (see Saffer and Tobin, 2011), we briefly discuss some aspects of sediment hydrology here.

Sediment composition strongly controls its hydrologic character, because clayey sediments are known to have very low permeability (e.g., Domenico and Mifflin, 1965; Mitchell et al., 1965; Neuzil, 1994). The measured permeability of smectites, in particular, is extremely low even compared to other clay species (e.g., Levy et al., 1993; Revil and Cathles, 1999; Ikari et al., 2009; Behnsen and Faulkner, 2011). Because of this, compared to quartz-rich silty or sandy sediments, clays dewater more slowly under compression and are prone to developing excess pore pressures. Sediment diagenesis can also lead to excess pore pressures because common reactions such as opal to quartz and smectite dehydration release mineral-bound water (Colten-Bradley, 1987; Fitts and Brown, 1999; Bekins et al., 1994; Kastner et al., 2014).

Results of numerical fluid flow modeling for the Muroto transect at the Nankai Trough indicated a zone of excess pore pressure and minimum effective stress in the upper hemipelagic unit of the incoming sediment, which is broadly consistent with the horizon of the proto-décollement zone at Site 1173

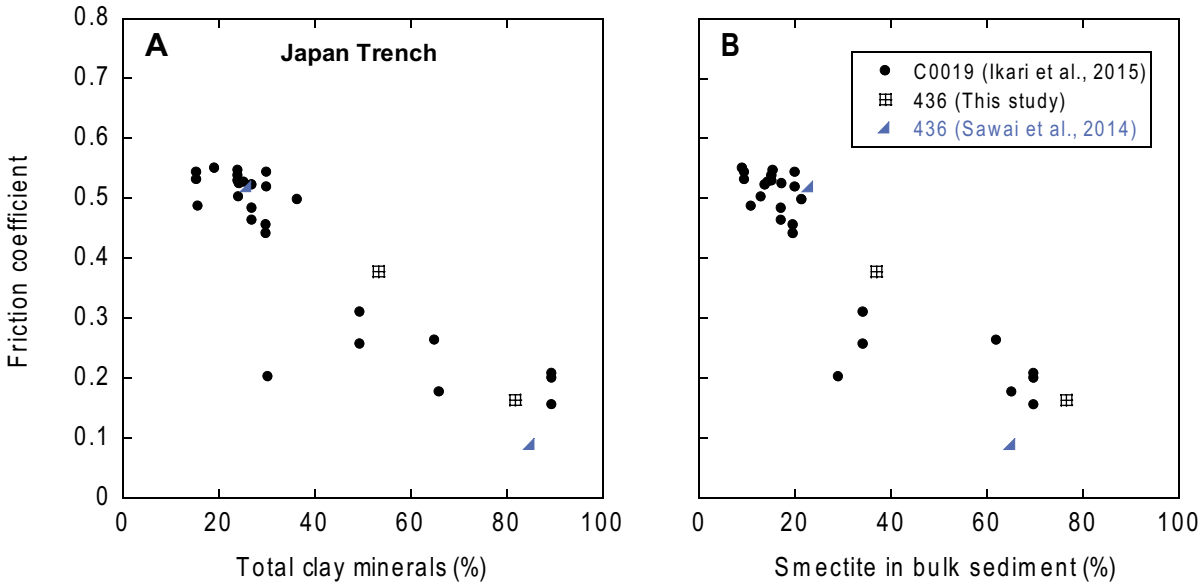

Figure 13. Friction coefficient as a function of total clay minerals (A) and smectite content in the bulk sediment (B) for the Japan Trench drilling sites (see Fig. 7 for locations). Mineral content data are from Shipboard Scientific Party (1980) and Kameda et al. (2015a). Note that for some samples, clay and smectite contents are not available (see Table 2).

(Le Pichon et al., 1993; Skarbek and Saffer, 2009). Because friction experiments show that the hemipelagic clay portion of the LSB facies is relatively homogeneous in mechanical character, pore pressure patterns likely play a relatively important role in controlling incipient deformation at the toe at this particular location as suggested by previous studies (e.g., Taira et al., 1992; Screaton et al., 2002; Brown et al., 2003; Kopf and Brown, 2003; Tobin and Saffer, 2009). On the other hand, for the erosional Costa Rican margin, integration of laboratory consolidation tests and downhole drilling data show that excess pore pressures and a minimum in effective stress should have developed ~100 m deep in the underthrust section (Saffer, 2003). Despite this, the décollement is localized in the top of the subducting sediment section, consistent with observations of lower coefficients of friction for the hemipelagic section. This suggests that in the Costa Rica subduction zone, the mineralogical composition has a dominant role in controlling the décollement position rather than hydrologic effects.

SUMMARY AND CONCLUSIONS

Based on laboratory friction experiments and XRD data from scientific drilling samples, we analyze the role of mineralogic composition for input sediments to the Nankai Trough, Japan Trench, and Costa Rica subduction zones. Both the Japan Trench and Costa Rica subduction zones exhibit a negative dependence of friction coefficient on bulk clay content, consistent with earlier laboratory work. Smectite is a key mineral in the Japan Trench, where a smectite-rich pelagic clay exhibits very low friction. This smectite layer is the origin of the eventual plate boundary and hosted the 2011 Tohoku-Oki earthquake. At Costa Rica, pelagic nannofossil oozes and chalks have high frictional strength, which contrasts with the weaker hemipelagic clay-rich sediment. This helps explain the small amount of offscraping at the deformation front, enhanced subduction erosion where the hemipelagic sediment is absent, and why nearly the entire sediment package is subducted at the Middle America Trench.

The Nankai Trough is significantly more complicated, due to an observed wide range of friction coefficients that does not correlate with either bulk clay content or smectite content. As a consequence, this has probably led to significant along-strike variability in plate boundary position and taper angle of the wedge. Because the strength contrasts between different lithologic units in the Nankai Trough are not as clear as those in the Japan Trench and at Costa Rica, we infer that secondary processes influence mechanical behavior. These include effects of sediment diagenesis and hydrologic effects which cause pore fluid pressure variations. We conclude that for an individual subduction zone, mechanical behavior may be explained by the mineral assemblage and spatial distribution of

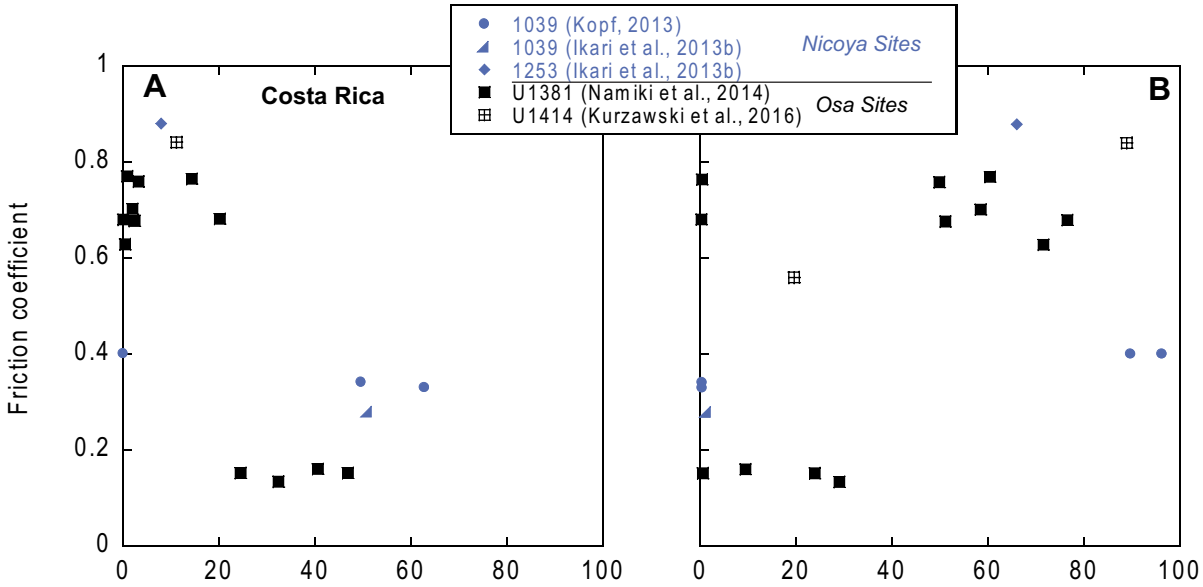

Figure 14. Friction coefficient as a function of total clay minerals (A) and calcite content (B) for the Middle America Trench drilling sites, offshore Costa Rica (see Fig. 9 for locations). Mineral content data are from Ikari et al. (2013b), Kameda et al. (2015b), and Kurzawski et al. (2016).

key minerals in the sediment inputs. Given that these may vary widely from margin to margin, it is appropriate to analyze each subduction zone as a unique case.

ACKNOWLEDGMENTS

We thank Jun Kameda, Yuka Namiki, and Akito Tsutsumi for providing access to their data, and Hugues Raimbourg and Michael Stipp for providing helpful reviews. This work was supported by the Deutsche Forschungsgemeinschaft via MARUM Research Center (grants FZT15 and EXC309), and via project HU 1789/3-1 to AH.

REFERENCES CITED

Adams, J., 1990, Paleoseismicity of the Cascadia subduction zone: Evidence from turbidites off the Oregon-Washington margin: Tectonics, v. 9, p. 569–583, https://doi.org/10.1029/TC009i004p00569.

Ando, M., 1975, Source mechanisms and tectonic significance of historical earthquakes along the Nankai Trough, Japan: Tectonophysics, v. 27, p. 119–140, https://doi.org/10.1016/0040-1951(75)90102-X.

Arthur, M.A., and Adelseck, C.G., Jr., 1980, Acknowledgements, introduction, and explanatory notes: The Japan Trench transect, Legs 56 and 57, Deep Sea Drilling Project, *in* Scientific Party, Initial Reports of the Deep Sea Drilling Project, Volume 56, 57, Part 1: Washington, D.C., U.S. Government Printing Office, p. 3–21, https://doi.org/10.2973/dsdp.proc.5657.101.1980.

Barckhausen, U., Ranero, C.R., von Huene, R., Cande, S.C., and Roeser, H.A., 2001, Revised tectonic boundaries for the Cocos Plate off Costa Rica: Implications for the segmentation of the convergent margin and for plate tectonic models: Journal of Geophysical Research, v. 106, p. 19,207–19,220, https://doi.org/10.1029/2001JB000238.

Behnsen, J., and Faulkner, D.R., 2011, Water and argon permeability of phyllosilicate powders under medium to high pressure: Journal of Geophysical Research, v. 116, B12203, https://doi.org/10.1029/2011JB008600.

Bekins, B., McCaffrey, A.M., and Dreiss, S.J., 1994, Influence of kinetics on the smectite to illite transition in the Barbados accretionary prism: Journal of Geophysical Research, v. 99, p. 18,147–18,158, https://doi.org/10.1029/94JB01187.

Bilek, S.L., 2007, Influence of subducting topography on earthquake rupture, *in* Dixon, T.H., and Moore, J.C., eds., The Seismogenic Zone of Subduction Thrust Faults: New York, Columbia University Press, p. 123–146, https://doi.org/10.7312/dixo13866-005.

Bourlange, S., Jouniax, L., and Henry, P., 2004, Data report: Permeability, compressibility, and friction coefficient measurements under confining pressure and strain, Leg 190, Nankai Trough, *in* Mikada, H., Moore, G.F., Taira, A. Becker, K., Moore, J.C. and Klaus, A., eds., Proceedings of the Ocean Drilling Program, Scientific Results, Volume 190/196: College Station, Texas, Ocean Drilling Program, 16 p., https://doi.org/10.2973/odp.proc.sr.190196.215.2004.

Brown, K.M., Kopf, A.J., Underwood, M.B., and Weinberger, J.L., 2003, Compositional and fluid pressure controls on the state of stress on the Nankai subduction thrust: A weak plate boundary: Earth and Planetary Science Letters, v. 214, p. 589–603, https://doi.org/10.1016/S0012-821X(03)00388-1.

Byerlee, J., 1978, Friction of rocks: Pure and Applied Geophysics, v. 116, p. 615–626, https://doi.org/10.1007/BF00876528.

Chester, F.M., Mori, J.J., Eguchi, N., Toczko, S., and the Expedition 343/343T Scientists, 2013a, Proceedings of the Integrated Ocean Drilling Program, Volume 343/343T: Tokyo, Inte-

grated Ocean Drilling Program Management International, Inc., https://doi.org/10.2204/iodp.proc.343343T.2013.

Chester, F.M., Rowe, C., Ujiie, K., Kirkpatrick, J., Regalla, C., Remitti, F., Moore, J.C., Toy, V., Wolfson-Schwehr, M., Bose, S., Kameda, J., Mori, J.J., Brodsky, E.E., Eguchi, N., Toczko, S., and Expedition 343 and 343T Scientists, 2013b, Structure and composition of the plate-boundary slip zone for the 2011 Tohoku-Oki earthquake: Science, v. 342, p. 1208–1211, https://doi.org/10.1126/science.1243719.

Colten-Bradley, V.A., 1987, Role of pressure in smectite dehydration—Effects on geopressure and smectite-to-illite transformation: American Association of Petroleum Geologists Bulletin, v. 71, p. 1414–1427.

Costa Pisani, P., Reshef, M., and Moore, G., 2005, Targeted 3-D prestack depth imaging at Legs 190–196 ODP drill sites (Nankai Trough, Japan): Geophysical Research Letters, v. 32, L20309, https://doi.org/10.1029/2005GL024191.

Crawford, B.R., Faulkner, D.R., and Rutter, E.H., 2008, Strength, porosity, and permeability development during hydrostatic and shear loading of synthetic quartz-clay fault gouge: Journal of Geophysical Research, v. 113, B03207, https://doi.org/10.1029/2006JB004634.

Dahlen, F.A., 1990, Critical taper model of fold-and-thrust belts and accretionary wedges: Annual Review of Earth and Planetary Sciences, v. 18, p. 55–99, https://doi.org/10.1146/annurev.ea.18.050190.000415.

Davis, D., Suppe, J., and Dahlen, F.A., 1983, Mechanics of fold-and-thrust belts and accretionary wedges: Journal of Geophysical Research, v. 88, p. 1153–1172, https://doi.org/10.1029/JB088iB02p01153.

DeMets, C., Gordon, R.G., and Argus, D.F., 2010, Geologically current plate motions: Geophysical Journal International, v. 181, p. 1–80, https://doi.org/10.1111/j.1365-246X.2009.04491.x.

Deng, X., and Underwood, M.B., 2001, Abundance of smectite and the location of a plate-boundary fault, Barbados accretionary prism: Geological Society of America Bulletin, v. 113, p. 495–507, https://doi.org/10.1130/0016-7606(2001)113<0495:AOSATL>2.0.CO;2.

Di Toro, G., Han, R., Hirose, T., De Paola, N., Nielsen, S., Mizoguchi, K., Ferri, F., Cocco, M., and Shimamoto, T., 2011, Fault lubrication during earthquakes: Nature, v. 471, p. 494–498, https://doi.org/10.1038/nature09838.

Domenico, P.A., and Mifflin, M.D., 1965, Water from low-permeability sediments and land subsidence: Water Resources Research, v. 1, p. 563–576, https://doi.org/10.1029/WR001i004p00563.

Expedition 333 Scientists, 2012a, Site C0011, *in* Henry, P., Kanamatsu, T., More, K., and the Expedition 333 Scientists, Proceedings of the Integrated Ocean Drilling Program, Volume 333: Tokyo, Integrated Ocean Drilling Program Management International, Inc., https://doi.org/10.2204/iodp.proc.333.104.2012.

Expedition 333 Scientists, 2012b, Site C0012, *in* Henry, P., Kanamatsu, T., More, K., and the Expedition 333 Scientists, Proceedings of the Integrated Ocean Drilling Program, Volume 333: Tokyo, Integrated Ocean Drilling Program Management International, Inc., https://doi.org/10.2204/iodp.proc.333.105.2012.

Fisher, A.T., Stein, C.A., Harris, R.N., Wang, K., Silver, E.A., Pfender, M., Hutnak, M., Cherkaoui, A., Bodzin, R., and Villinger, H., 2003, Abrupt thermal transition reveals hydrothermal boundary and role of seamounts within the Cocos Plate: Geophysical Research Letters, v. 30, 1550, https://doi.org/10.1029/2002GL016766.

Fitts, T.G., and Brown, K.M., 1999, Stress-induced smectite dehydration: Ramifications for patterns of freshening and fluid expulsion in the N. Barbados accretionary wedge: Earth and Planetary Science Letters, v. 172, p. 179–197, https://doi.org/10.1016/S0012-821X(99)00168-5.

Fulton, P.F., Brodsky, E.E., Kano, Y., Mori, J., Chester, F., Ishikawa, T., Harris, R.N., Lin, W., Eguchi, N., Toczko, S., and Expedition 343, 343T, and KR13-08 Scientists, 2013, Low coseismic friction on the Tohoku-Oki fault determined from temperature measurements: Science, v. 342, p. 1214–1217, https://doi.org/10.1126/science.1243641.

Goldfinger, C., Kulm, L.D., McNeill, L.C., and Watts, P., 2000, Super-scale failure of the southern Oregon Cascadia margin: Pure and Applied Geophysics, v. 157, p. 1189–1226, https://doi.org/10.1007/s000240050023.

Harris, R.N., Grevemeyer, I., Ranero, C.R., Villinger, H., Barckhausen, U., Henke, T., Mueller, C., and Neben, S., 2010a, Thermal regime of the Costa Rica convergent margin: 1. Along-strike variations in heat flow from probe measurements and estimated from bottom-simulating reflectors: Geochemistry Geophysics Geosystems, v. 11, Q12S28, https://doi.org/10.1029/2010GC003272.

Harris, R.N., Spinelli, G., Ranero, C.R., Grevemeyer, I., Villinger, H., and Barckhausen, U., 2010b, Thermal regime of the Costa Rica convergent margin: 2. Thermal models of the shallow Middle America subduction zone offshore Costa Rica: Geochemistry Geophysics Geosystems, v. 11, Q12S29, https://doi.org/10.1029/2010GC003273.

Harris, R.N., Yamano, M., Kinoshita, M., Spinelli, G., Hamamoto, H., and Ashi, J., 2013a, A synthesis of heat flow determinations and thermal modeling along the Nankai Trough, Japan: Journal of Geophysical Research: Solid Earth, v. 118, p. 2687–2702, https://doi.org/10.1002/jgrb.50230.

Harris, R.N., Sakaguchi, A., Petronotis, K., and the Expedition 344 Scientists, 2013b, Proceedings of the Integrated Ocean Drilling Program, Volume 344: College Station, Texas, Integrated Ocean Drilling Program, https://doi.org/10.2204/iodp.proc.344.2013.

Henry, P., Kanamatsu, T., Moe, K., and the Expedition 333 Scientists, 2012, Proceedings of the Integrated Ocean Drilling Program, Volume 333: Tokyo, Integrated Ocean Drilling Program Management International, Inc., https://doi.org/10.2204/iodp.proc.333.2012.

Hey, R., 1977, Tectonic evolution of the Cocos-Nazca spreading center: Geological Society of America Bulletin, v. 88, p. 1404–1420, https://doi.org/10.1130/0016-7606(1977)88<1404:TEOTCS>2.0.CO;2.

Hinz, K., von Huene, R., Ranero, C.R., and the PACOMAR Working Group, 1996, Tectonic structure of the convergent Pacific margin offshore Costa Rica from multichannel seismic reflection data: Tectonics, v. 15, p. 54–66, https://doi.org/10.1029/95TC02355.

Hodder, A.P.W., Naish, T.R., and Nelson, C.S., 1993, A two-stage model for the formation of smectite from detrital volcanic glass under shallow-marine conditions: Marine Geology, v. 109, p. 279–285, https://doi.org/10.1016/0025-3227(93)90066-5.

Hüpers, A., Ikari, M.J., Dugan, B., Underwood, M.B., and Kopf, A.J., 2015, Origin of a zone of anomalously high porosity in the subduction inputs to Nankai Trough: Marine Geology, v. 361, p. 147–162, https://doi.org/10.1016/j.margeo.2015.01.004.

Husen, S., Kissling, E., and Quintero, R., 2002, Tomographic evidence for a subducted seamount beneath the Gulf of Nicoya, Costa Rica: The cause of the 1990 Mw = 7.0 Gulf of Nicoya earthquake: Geophysical Research Letters, v. 29, p. 79-1–79-4, https://doi.org/10.1029/2001GL014045.

Ikari, M.J., 2015, Data report: Rate- and state-dependent friction parameters of core samples from Site C0019, IODP Expedition 343 (JFAST), *in* Chester, F.M., Mori, J., Eguchi, N., Toczko, S., and the Expedition 343/343T Scientists: Proceedings of the Integrated Ocean Drilling Program, Volume 343/343T: Tokyo, Integrated Ocean Drilling Program Management International, Inc., https://doi.org/10.2204/iodp.proc.343343T.203.2015.

Ikari, M.J., and Saffer, D.M., 2011, Comparison of frictional strength and velocity dependence between fault zones in the Nankai accretionary complex: Geochemistry Geophysics Geosystems, v. 12, Q0AD11, doi:10.1029/2010GC003442.

Ikari, M.J., Saffer, D.M., and Marone, C., 2007, Effect of hydration state on the frictional properties of montmorillonite-based fault gouge: Journal of Geophysical Research, v. 112, B06423, https://doi.org/10.1029/2006JB004748.

Ikari, M.J., Saffer, D.M., and Marone, C., 2009, Frictional and hydrologic properties of clay-rich fault gouge: Journal of Geophysical Research, v. 114, B05409, https://doi.org/10.1029/2008JB006089.

Ikari, M.J., Hüpers, A., and Kopf, A.J., 2013a, Shear strength of sediments approaching subduction in the Nankai Trough, Japan as constraints on forearc mechanics: Geochemistry Geophysics Geosystems, v. 14, p. 2716–2730, https://doi.org/10.1002/ggge.20156.

Ikari, M.J., Niemeijer, A.R., Spiers, C.J., Kopf, A.J., and Saffer, D.M., 2013b, Experimental evidence linking slip instability with seafloor lithology and topography at the Costa Rica convergent margin: Geology, v. 41, p. 891–894, https://doi.org/10.1130/G33956.1.

Ikari, M.J., Kameda, J., Saffer, D.M., and Kopf, A.J., 2015, Strength characteristics of Japan Trench borehole samples in the high-slip region of the 2011 Tohoku-Oki earthquake: Earth and Planetary Science Letters, v. 412, p. 35–41, https://doi.org/10.1016/j.epsl.2014.12.014.

Ito, Y., Tsuji, T., Osada, Y., Kido, M., Inazu, D., Hayashi, Y., Tsushima, H., Hino, R., and Fujimoto, H., 2011, Frontal wedge deformation near the source region of the 2011 Tohoku-Oki earthquake: Geophysical Research Letters, v. 38, L00G05, https://doi.org/10.1029/2011GL048355.

Kameda, J., Shimizu, M., Ujiie, K., Hirose, T., Ikari, M., Mori, J., Oohashi, K., and Kimura, G., 2015a, Pelagic smectite as an important factor in tsunamigenic slip along the Japan Trench: Geology, v. 43, p. 155–158, https://doi.org/10.1130/G35948.1.

Kameda, J., Harris, R.N., Shimizu, M., Ujiie, K., Tsutsumi, A., Ikehara, M., Uno, M., Yamaguchi, A., Hamada, Y., Namiki, Y., and Kimura, G., 2015b, Hydrogeological responses to incoming materials at the erosional subduction margin, offshore Osa Peninsula, Costa Rica: Geochemistry Geophysics Geosystems, v. 16, p. 2725–2742, https://doi.org/10.1002/2015GC005837.

Kastner, M., Soloman, E.A., Harris, R.N., and Torres, M.E., 2014, Fluid origins, thermal regimes, and fluid and solute fluxes in the forearc of subduction zones, *in* Stein, R., Blackman, D.K., Inagaki, F., and Larsen, H.-C., eds., Earth and Life Processes Discovered from Subseafloor Environments: A Decade of Science Achieved by the Integrated Ocean Drilling Program (IODP):

Developments in Marine Geology, v. 7: Amsterdam, Netherlands, Elsevier, p. 671–733, https://doi.org/10.1016/B978-0-444-62617-2.00022-0.
Kikuchi, M., Nakamura, M., and Yoshikawa, K., 2003, Source rupture processes of the 1944 Tonankai earthquake and the 1945 Mikawa earthquake derived from low-gain seismograms: Earth, Planets, and Space, v. 55, p. 159–172, https://doi.org/10.1186/BF03351745.
Kimura, G., Silver, E.A., Blum, P., et al., 1997, Proceedings of the Ocean Drilling Program, Initial Reports, Volume 170: College Station, Texas, Ocean Drilling Program, https://doi.org/10.2973/odp.proc.ir.170.1997.
Kimura, G., Kitamura, Y., Hashimoto, Y., Yamaguchi, A., Shibata, T., Ujiie, K., and Okamoto, S., 2007, Transition of accretionary wedge structures around the up-dip limit of the seismogenic subduction zone: Earth and Planetary Science Letters, v. 255, p. 471–484, https://doi.org/10.1016/j.epsl.2007.01.005.
Kimura, G., Screaton, E.J., Curewitz, D., and the Expedition 316 Scientists, 2008, NanTroSEIZE Stage 1A: NanTroSEIZE shallow megasplay and frontal thrusts: Integrated Ocean Drilling Program Preliminary Report, Volume 316: Washington, D.C., Integrated Ocean Drilling Program Management International, Inc., https://doi.org/10.2204/iodp.pr.316.2008.
Kinoshita, M., Kanamatsu, T., Kawamura, K., Shibata, T., Hamamoto, H., and Fujino, K., 2008, Heat flow distribution on the floor of Nankai Trough off Kumano and implications for the geothermal regime of subducting sediments: Japan Agency for Marine-Earth Science and Technology Report of Research and Development, v. 8, p. 13–28.
Kirkpatrick, J.D., Rowe, C.D., Ujiie, K., Moore, J.C., Regalla, C., Remitti, F., Toy, V., Wolfson-Schwehr, M., Kameda, J., Bose, S., and Chester, F.M., 2015, Structure and lithology of the Japan Trench subduction plate boundary fault: Tectonics, v. 34, p. 53–69, https://doi.org/10.1002/2014TC003695.
Kitamura, Y., and Yamamoto, Y., 2012, Records of submarine landslides in subduction input recovered by IODP Expedition 322, Nankai Trough, Japan, *in* Yamada, Y., Kawamura, K., Ikehara, K., Ogawa, Y., Urgeles, R., Mosher, D., Chaytor, J., and Strasser, M., eds., Submarine Mass Movements and their Consequences: 5th International Symposium: Advances in Natural and Technological Hazards Research, v. 31: Switzerland, Springer International Publishing, p. 659–670, https://doi.org/10.1007/978-94-007-2162-3_59.
Kopf, A., 2013, Effective strength of incoming sediments and its implications for plate boundary propagation: Nankai and Costa Rica as type examples of accreting vs. erosive convergent margins: Tectonophysics, v. 608, p. 958–969, https://doi.org/10.1016/j.tecto.2013.07.023.
Kopf, A., and Brown, K.M., 2003, Friction experiments on saturated sediments and their implications for the stress state of the Nankai and Barbados subduction thrusts: Marine Geology, v. 202, p. 193–210, https://doi.org/10.1016/S0025-3227(03)00286-X.
Kurzawski, R.M., Stipp, M., Niemeijer, A.R., Spiers, C.J., and Behrmann, J.H., 2016, Earthquake nucleation in weak subducted carbonates: Nature Geoscience, v. 9, p. 717–722, https://doi.org/10.1038/ngeo2774.
Le Pichon, X., Henry, P., and Lallemant, S., 1993, Accretion and erosion in subduction zones: The role of fluids: Annual Review of Earth and Planetary Sciences, v. 21, p. 307–331, https://doi.org/10.1146/annurev.ea.21.050193.001515.
Levy, G.J., Eisenberg, H., and Shainberg, I., 1993, Clay dispersion as related to soil properties and water permeability: Soil Science, v. 155, p. 15–22, https://doi.org/10.1097/00010694-199301000-00003.
Logan, J.M., and Rauenzahn, K.A., 1987, Frictional dependence of gouge mixtures of quartz and montmorillonite on velocity, composition, and fabric: Tectonophysics, v. 144, p. 87–108, https://doi.org/10.1016/0040-1951(87)90010-2.
Loveless, J.P., and Meade, B.J., 2010, Geodetic imaging of plate motions, slip rate, and partitioning of deformation in Japan: Journal of Geophysical Research, v. 115, B02410, https://doi.org/10.1029/2008JB006248.
Lupini, J.F., Skinner, A.E., and Vaughan, P.R., 1981, The drained residual strength of cohesive soils: Geotechnique, v. 31, p. 181–213, https://doi.org/10.1680/geot.1981.31.2.181.
MacKay, M.E., 1995, Structural variation and landward vergence at the toe of the Oregon accretionary prism: Tectonics, v. 14, p. 1309–1320, https://doi.org/10.1029/95TC02320.
Masson, D.G., Harbitz, C.B., Wynn, R.B., Pedersen, G., and Løvholt, F., 2006, Submarine landslides: Processes, triggers and hazard prediction: Philosophical Transactions of the Royal Society of London A, v. 364, p. 2009–2039, https://doi.org/10.1098/rsta.2006.1810.
Masuda, H., O'Neil, J.R., Jiang, W.-T., and Peacor, D.R., 1996, Relation between interlayer composition of authigenic smectite, mineral assemblages, I/S reaction rate and fluid composition in silicic ash of the Nankai Trough: Clays and Clay Minerals, v. 44, p. 443–459, https://doi.org/10.1346/CCMN.1996.0440402.
Meschede, M., Zwiegel, P., and Kiefer, E., 1999, Subsidence and extension at a convergent plate margin: Evidence for subduction erosion off Costa Rica: Terra Nova, v. 11, p. 112–117, https://doi.org/10.1046/j.1365-3121.1999.00234.x.
Mitchell, J.K., Hooper, D.R., and Campanella, R.G., 1965, Permeability of compacted clay: Journal of the Soil Mechanics and Foundations Division, American Society of Civil Engineers, v. 91, p. 41–66.
Miyazaki, S., and Heki, K., 2001, Crustal velocity field of southwest Japan: Subduction and arc-arc collision: Journal of Geophysical Research, v. 106, p. 4305–4326, https://doi.org/10.1029/2000JB900312.
Moore, D.E., and Lockner, D.A., 2007, Friction of the smectite clay montmorillonite: A review and interpretation of data, *in* Dixon, T.H., and Moore, J.C., eds., The Seismogenic Zone of Subduction Thrust Faults: New York, Columbia University Press, p. 317–345, https://doi.org/10.7312/dixo13866-011.
Moore, G.F., Taira, A., Klaus, A., Becker, L., Boeckel, B., Cragg, B.A., Dean, A., Fergusson, C.L., Henry, P., Hirano, S., Hisamitsu, T., Hunze, S., Kastner, M., Maltman, A.J., Morgan, J.K., Murakami, Y., Saffer, D.M., Sánchez-Gomez, M., Screaton, E.J., Smith, D.C., Spivack, A.J., Steurer, J., Tobin, H.J., Ujiie, K., Underwood, M.B., and Wilson, M., 2001, New insights into deformation and fluid flow processes in the Nankai Trough accretionary prism: Results of Ocean Drilling Program Leg 190: Geochemistry Geophysics Geosystems, v. 2, 1058, https://doi.org/10.1029/2001GC000166.
Moore, G.F., Park, J.-O., Bangs, N.L., Gulick, S.P., Tobin, H.J., Nakamura, Y., Sato, S., Tsuji, T., Yoro, T., Tanaka, H., Uraki, S., Kido, Y., Sanada, Y., Kuramoto, S., and Taira, A., 2009, Structural and seismic framework of the NanTroSEIZE Stage 1 transect, *in* Kinoshita, M., Tobin, H., Ashi, J., Kimura, G., Lallemant, S., Screaton, E.J., Curewitz, D., Masago, H., Moe, K.T., and the Expedition 314/315/316 Scientists, Proceedings of the Integrated Ocean Drilling Program, Volume 314/315/316: Washington, D.C., Integrated Ocean Drilling Program Management International, Inc., https://doi.org/10.2204/iodp.proc.314315316.102.2009.
Moore, J.C., 1989, Tectonics and hydrogeology of accretionary prisms: Role of the décollement zone: Journal of Structural Geology, v. 11, p. 95–106, https://doi.org/10.1016/0191-8141(89)90037-0.
Moore, J.C., and Saffer, D.M., 2001, Updip limit of the seismogenic zone beneath the accretionary prism of southwest Japan: An effect of diagenetic to low-grade metamorphic processes and increasing effective stress: Geology, v. 29, p. 183–186, https://doi.org/10.1130/0091-7613(2001)029<0183:ULOTSZ>2.0.CO;2.
Moore, J.C., Moore, G.F., Cochrane, G.R., and Tobin, H.J., 1995, Negative-polarity seismic reflections along faults of the Oregon accretionary prism: Indicators of overpressuring: Journal of Geophysical Research, v. 100, p. 12,895–12,906, https://doi.org/10.1029/94JB02049.
Moore, J.C., Klaus, A., Bangs, N.L., Bekins, B., Bücker, C.J., Brückmann, W., Erickson, S.E., Hansen, O., Horton, T., Ireland, P., Major, C.O., Moore, G.F., Peacock, S., Saito, S., Screaton, E.J., Shimeld, J.W., Stauffer, P.H., Taymaz, T., Teas, P.A., and Tokunaga, T., 1998, Consolidation patterns during initiation and evolution of a plate-boundary decollement zone: Northern Barbados accretionary prism: Geology, v. 26, p. 811–814, https://doi.org/10.1130/0091-7613(1998)026<0811:CPDIAE>2.3.CO;2.
Moore, J.C., Rowe, C., and Meneghini, F., 2007, How accretionary prisms elucidate seismogenesis in subduction zones, *in* Dixon, T.H., and Moore, J.C., eds., The Seismogenic Zone of Subduction Thrust Faults: New York, Columbia University Press, p. 288–315, https://doi.org/10.7312/dixo13866-010.
Moore, J.C., Plank, T.A., Chester, F.M., Polissar, P.J., and Savage, H.M., 2015, Sediment provenance and controls on slip propagation: Lessons learned from the 2011 Tohoku and other great earthquakes of the subducting northwest Pacific plate: Geosphere, v. 11, p. 533–541, https://doi.org/10.1130/GES01099.1.
Morris, J.D., Villinger, H.W., Klaus, A., et al., 2003, Proceedings of the Ocean Drilling Program, Initial Reports, Volume 205: College Station, Texas, Ocean Drilling Program, https://doi.org/10.2973/odp.proc.ir.205.2003.
Morrow, C., Radney, B., and Byerlee, J., 1992, Frictional strength and the effective pressure law of montmorillonite and illite clays, *in* Evans, B., and Wong, T.-F., eds., Fault Mechanics and Transport Properties of Rocks A Festschrift in Honor of W.F. Brace: London, Academic Press, International Geophysics, v. 51, p. 69–88, https://doi.org/10.1016/S0074-6142(08)62815-6.
Morrow, C.A., Moore, D.E., and Lockner, D.A., 2000, The effect of mineral bond strength and adsorbed water on fault gouge frictional strength: Geophysical Research Letters, v. 27, p. 815–818, https://doi.org/10.1029/1999GL008401.
Namiki, Y., Tsutsumi, A., Ujiie, K., and Kameda, J., 2014, Frictional properties of sediments entering the Costa Rica subduction zone offshore the Osa Peninsula: Implications for fault slip in shallow subduction zones: Earth, Planets, and Space, v. 66, 72, https://doi.org/10.1186/1880-5981-66-72.

Neuzil, C.E., 1994, How permeable are clays and shales?: Water Resources Research, v. 30, p. 145–150, https://doi.org/10.1029/93WR02930.

Pickering, K.T., Underwood, M.B., and Taira, A., 1993, Stratigraphic synthesis of the DSDP-ODP sites in the Shikoku Basin, Nankai Trough, and accretionary prism, *in* Hill, I.A., Taira, A., Firth, J.V., et al., eds., Proceedings of the Ocean Drilling Program, Scientific Results, Volume 131: College Station, Texas, Ocean Drilling Program, p. 313–330, https://doi.org/10.2973/odp.proc.sr.131.135.1993.

Polet, J., and Kanamori, H., 2000, Shallow subduction zone earthquakes and their tsunamigenic potential: Geophysical Journal International, v. 142, p. 684–702, https://doi.org/10.1046/j.1365-246x.2000.00205.x.

Protti, M., McNally, K., Pacheco, J., González, V., Montero, C., Segura, J., Brenes, J., Barboza, V., Malavassi, E., Güendel, F., Simila, G., Rojas, D., Velasco, A., Mata, A., and Schillinger, W., 1995, The March 25, 1990 (M_w=7.0, M_L=6.8), earthquake at the entrance of the Nicoya Gulf, Costa Rica: Its prior activity, foreshocks, aftershocks, and triggered seismicity: Journal of Geophysical Research, v. 100, p. 20,345–20,358, https://doi.org/10.1029/94JB03099.

Pytte, A.M., and Reynolds, R.C., 1989, The thermal transition of smectite to illite, *in* Naeser, N.D., and McCulloch, T.H., eds., Thermal History of Sedimentary Basins: Methods and Case Studies: New York, Springer, p. 133–140, https://doi.org/10.1007/978-1-4612-3492-0_8.

Raimbourg, H., Hamano, Y., Saito, S., Kinoshita, M., and Kopf, A., 2011, Acoustic and mechanical properties of Nankai accretionary prism core samples: Geochemistry Geophysics Geosystems, v. 12, Q0AD10, https://doi.org/10.1029/2010GC003169.

Ranero, C.R., and von Huene, R., 2000, Subduction erosion along the Middle America convergent margin: Nature, v. 404, p. 748–752, https://doi.org/10.1038/35008046.

Rea, D.K., and Ruff, L.J., 1996, Composition and mass flux of sediment entering the world's subduction zones: Implications for global sediment budgets, great earthquakes, and volcanism: Earth and Planetary Science Letters, v. 140, p. 1–12, https://doi.org/10.1016/0012-821X(96)00036-2.

Remitti, F., Smith, S.A.F., Mittempergher, S., Gualtieri, A.F., and Di Toro, G., 2015, Frictional properties of fault zone gouges from the J-FAST drilling project (Mw 9.0 Tohoku-Oki earthquake): Geophysical Research Letters, v. 42, p. 2691–2699, https://doi.org/10.1002/2015GL063507.

Revil, A., and Cathles, L.M., 1999, Permeability of shaly sands: Water Resources Research, v. 35, p. 651–662, https://doi.org/10.1029/98WR02700.

Saffer, D.M., 2003, Pore pressure development and progressive dewatering in underthrust sediments at the Costa Rican subduction margin: Comparison with northern Barbados and Nankai: Journal of Geophysical Research, v. 108, 2261, https://doi.org/10.1029/2002JB001787.

Saffer, D.M., and Tobin, H.J., 2011, Hydrogeology and mechanics of subduction zone forearcs: Fluid flow and pore pressure: Annual Reviews of Earth and Planetary Science, v. 39, 157–186, https://doi.org/10.1146/annurev-earth-040610-133408.

Saffer, D.M., Underwood, M.B., and McKiernan, A.W., 2008, Evaluation of factors controlling smectite transformation and fluid production in subduction zones: Application to the Nankai Trough: The Island Arc, v. 17, p. 208–230, https://doi.org/10.1111/j.1440-1738.2008.00614.x.

Saffer, D.M., Lockner, D.A., and McKiernan, A., 2012, Effects of smectite to illite transformation on the frictional strength and sliding stability of intact marine mudstones: Geophysical Research Letters, v. 39, L11304, https://doi.org/10.1029/2012GL051761.

Saito, S., Underwood, M.B., Kubo, Y., and the Expedition 322 Scientists, 2010, Proceedings of the Integrated Ocean Drilling Program, Volume 322: Tokyo, Integrated Ocean Drilling Program Management International, Inc., https://doi.org/10.2204/iodp.proc.322.2010.

Sawai, M., Hirose, T., and Kameda, J., 2014, Frictional properties of incoming pelagic sediments at the Japan Trench: Implications for large slip at a shallow plate boundary during the 2011 Tohoku earthquake: Earth, Planets, and Space, v. 66, https://doi.org/10.1186/1880-5981-66-65.

Schumann, K., Stipp, M., Leiss, B., and Behrmann, J.H., 2014, Texture development in naturally compacted and experimentally deformed silty clay sediments from the Nankai Trench and Forearc, Japan: Tectonophysics, v. 636, p. 125–142, https://doi.org/10.1016/j.tecto.2014.08.005.

Screaton, E., Saffer, D., Henry, P., Hunze, S., and Leg 190 Shipboard Scientific Party, 2002, Porosity loss within the underthrust sediments of the Nankai accretionary complex: Implications for overpressures: Geology, v. 30, p. 19–22, https://doi.org/10.1130/0091-7613(2002)030<0019:PLWTUS>2.0.CO;2.

Shimamoto, T., and Logan, J.M., 1981a, Effects of simulated clay gouges on the sliding behavior of Tennessee sandstone: Tectonophysics, v. 75, p. 243–255, https://doi.org/10.1016/0040-1951(81)90276-6.

Shimamoto, T., and Logan, J.M., 1981b, Effects of simulated fault gouge on the sliding behavior of Tennessee sandstone: Nonclay gouges: Journal of Geophysical Research, v. 86, p. 2902–2914, https://doi.org/10.1029/JB086iB04p02902.

Shipboard Scientific Party, 1975, Site 297, *in* Karig, D.E., Ingle, J.C. Jr., et al., eds., Initial Reports of the Deep Sea Drilling Project, Volume 31: Washington, D.C., U.S. Government Printing Office, p. 275–316, https://doi.org/10.2973/dsdp.proc.31.108.1975.

Shipboard Scientific Party, 1980, Site 436: Japan Trench outer rise, Leg 65, in Scientific Party, Initial Reports of the Deep Sea Drilling Project, Volume 56, 57, Part 1: Washington, D.C., U.S. Government Printing Office, p. 399–446, https://doi.org/10.2973/dsdp.proc.5657.107.1980.

Shipboard Scientific Party, 2001a, Site 1177, *in* Moore, G.F., Taira, A., Klaus, A., et al., 2001, Proceedings of the Ocean Drilling Program, Initial Reports, Volume 190: College Station, Texas, Ocean Drilling Program, https://doi.org/10.2973/odp.proc.ir.190.108.2001.

Shipboard Scientific Party, 2001b, Site 1173, *in* Moore, G.F., Taira, A., Klaus, A., et al., 2001, Proceedings of the Ocean Drilling Program, Initial Reports, Volume 190: College Station, Texas, Ocean Drilling Program, https://doi.org/10.2973/odp.proc.ir.190.104.2001.

Shipley, T.H., McIntosh, K.D., Silver, E.A., and Stoffa, P.L., 1992, Three-dimensional seismic imaging of the Costa Rica accretionary prism: Structural diversity in a small volume of the lower slope: Journal of Geophysical Research, v. 97, p. 4439–4459, https://doi.org/10.1029/91JB02999.

Singer, A., and Müller, G., 1979, Diagenesis in argillaceous sediments: Developments in Sedimentology, v. 25, p. 115–212, https://doi.org/10.1016/S0070-4571(08)71045-8.

Skarbek, R.M., and Saffer, D.M., 2009, Pore pressure development beneath the décollement at the Nankai subduction zone: Implications for plate boundary strength and sediment dewatering: Journal of Geophysical Research, v. 114, B07401, https://doi.org/10.1029/2008JB006205.

Spinelli, G.A., and Underwood, M.B., 2004, Character of sediments entering the Costa Rica subduction zone: Implications for partitioning of water along the plate interface: The Island Arc, v. 13, p. 432–451, https://doi.org/10.1111/j.1440-1738.2004.00436.x.

Spinelli, G.A., Mozley, P.S., Tobin, H.J., Underwood, M.B., Hoffman, N.W., and Bellew, G.M., 2007, Diagenesis, sediment strength, and pore collapse in sediment approaching the Nankai Trough subduction zone: Geological Society of America Bulletin, v. 119, p. 377–390, https://doi.org/10.1130/B25920.1.

Steurer, J.F., and Underwood, M.B., 2005, Clay mineralogy of mudstones from the Nankai Trough reference Sites 1173 and 1177 and frontal accretionary prism Site 1174, *in* Mikada, H., Moore, G.F., Taira, A., Becker, K., Moore, J.C., and Klaus, A., eds., Proceedings of the Ocean Drilling Program, Scientific Results, Volume 190/196: College Station, Texas, Ocean Drilling Program, 25 p., https://doi.org/10.2973/odp.proc.sr.190196.211.2003.

Stipp, M., Rolfs, M., Kitamura, Y., Behrmann, J.H., Schumann, K., Schulte-Kortnack, D., and Feeser, V., 2013, Strong sediments at the deformation front, and weak sediments at the rear of the Nankai accretionary prism, revealed by triaxial deformation experiments: Geochemistry Geophysics Geosystems, v. 14, p. 4791–4810, https://doi.org/10.1002/ggge.20290.

Strasser, M., Moore, G.F., Kimura, G., Kopf, A.J., Underwood, M.B., Guo, J., and Screaton, E.J., 2011, Slumping and mass transport deposition in the Nankai fore arc: Evidence from IODP drilling and 3-D reflection seismic data: Geochemistry Geophysics Geosystems, v. 12, Q0AD13, https://doi.org/10.1029/2010GC003431.

Strasser, M., Henry, P., Kanamatsu, T., Thu, M.K., Moore, G.F., and IODP Expedition 333 Scientists, 2012, Scientific drilling of mass-transport deposits in the Nankai accretionary wedge: First results from IODP Expedition 333, *in* Yamada, Y., Kawamura, K., Ikehara, K., Ogawa, Y., Urgeles, R., Mosher, D., Chaytor, J., and Strasser, M., eds., Submarine Mass Movements and their Consequences: 5th International Symposium: Advances in Natural and Technological Hazards Research, v. 31: Switzerland, Springer International Publishing, p. 671–681, https://doi.org/10.1007/978-94-007-2162-3_60.

Summers, R., and Byerlee, J., 1977, A note on the effect of fault gouge composition on the stability of frictional sliding: International Journal of Rock Mechanics and Mining Sciences & Geomechanics Abstracts, v. 14, p. 155–160, https://doi.org/10.1016/0148-9062(77)90007-9.

Taira, A., Hill, I., Firth, J., Berner, U., Brückmann, W., Byrne, T., Chabernaud, T., Fisher, A., Foucher, J.-P., Gamo, T., Gieskes, J., Hyndman, R., Karig, D., Kastner, M., Kato, Y., Lallemant, S., Lu, R., Maltman, A., Moore, G., Moran, K., Olaffson, G., Owens, W., Pickering, K., Siena, F., Taylor, E., Underwood, M., Wilkinson, C., Yamano, M., and Zhang, J., 1992, Sediment deformation and hydrogeology of the Nankai Trough accretionary prism: Synthesis of shipboard results of ODP Leg 131: Earth and Planetary Science Letters, v. 109, p. 431–450, https://doi.org/10.1016/0012-821X(92)90104-4.

Tanioka, Y., and Satake, K., 2001, Detailed coseismic slip distribution of the 1944 Tonankai earthquake estimated from tsunami waveforms: Geophysical Research Letters, v. 28, p. 1075–1078, https://doi.org/10.1029/2000GL012284.

Tobin, H.J., and Saffer, D.M., 2009, Elevated fluid pressure and extreme mechanical weakness of a plate boundary thrust, Nankai Trough subduction zone: Geology, v. 37, p. 679–682, https://doi.org/10.1130/G25752A.1.

Towe, K.M., 1962, Clay mineral diagenesis as a possible source of silica cement in sedimentary rocks: Journal of Sedimentary Petrology, v. 32, p. 26–28, https://doi.org/10.1306/74D70C3B-2B21-11D7-8648000102C1865D.

Ujiie, K., Tanaka, H., Saito, T., Tsutsumi, A., Mori, J.J., Kameda, J., Brodsky, E.E., Chester, F.M., Eguchi, E., Toczko, S., and Expedition 343 and 343T Scientists, 2013, Low coseismic shear stress on the Tohoku-Oki megathrust determined from laboratory experiments: Science, v. 342, p. 1211–1214, https://doi.org/10.1126/science.1243485.

Underwood, M.B., 2007, Sediment inputs to subduction zones: Why lithostratigraphy and clay mineralogy matter, *in* Dixon, T.H., and Moore, J.C., eds., The Seismogenic Zone of Subduction Thrust Faults: New York, Columbia University Press, p. 42–85, https://doi.org/10.7312/dixo13866-003.

Underwood, M.B., and Guo, J., 2013, Data report: Clay mineral assemblages in the Shikoku Basin, NanTroSEIZE subduction inputs, IODP Sites C0011 and C0012, *in* Saito, S., Underwood, M.B., Kubo, Y., and the Expedition 322 Scientists, Proceedings of the Integrated Ocean Drilling Program, Volume 322: Tokyo, Integrated Ocean Drilling Program Management International, Inc., https://doi.org/10.2204/iodp.proc.322.202.2013.

Underwood, M.B., Basu, N., Steurer, J., and Udas, S., 2003, Data report: Normalization factors for semiquantitative X-ray diffraction analysis, with application to DSDP Site 297, Shikoku Basin, *in* Mikada, H., Moore, G.F., Taira, A., Becker, K., Moore, J.C., and Klaus, A., eds., Proceedings of the Ocean Drilling Program, Scientific Results, Volume 190/196: College Station, Texas, Ocean Drilling Program, 28 p., https://doi.org/10.2973/odp.proc.sr.190196.203.2003.

Vannucchi, P., Ranero, C.R., Galeotti, S., Straub, S.M., Scholl, D.W., and McDougall-Ried, K., 2003, Fast rates of subduction erosion along the Costa Rica Pacific margin: Implications for nonsteady rates of crustal recycling at subduction zones: Journal of Geophysical Research, v. 108, 2511, https://doi.org/10.1029/2002JB002207.

Vannucchi, P., Ujiie, K., Stroncik, N., Malinverno, A., and the Expedition 334 Scientists, 2012, Proceedings of the Integrated Ocean Drilling Program, Volume 334: College Station, Texas, Integrated Ocean Drilling Program, https://doi.org/10.2204/iodp.proc.334.2012.

Vogt, C., Lauterjung, J., and Fischer, R.X., 2002, Investigation of the clay fraction (<2 µm) of the Clay Minerals Society reference clays: Clays and Clay Minerals, v. 50, p. 388–400, https://doi.org/10.1346/000986002760833765.

von Huene, R., and Culotta, R., 1989, Tectonic erosion at the front of the Japan Trench convergent margin: Tectonophysics, v. 160, p. 75–90, https://doi.org/10.1016/0040-1951(89)90385-5.

von Huene, R., and Lallemand, S., 1990, Tectonic erosion along the Japan and Peru convergent margins: Geological Society of America Bulletin, v. 102, p. 704–720, https://doi.org/10.1130/0016-7606(1990)102<0704:TEATJA>2.3.CO;2.

von Huene, R., Ranero, C.R., Weinrebe, W., and Hinz, K., 2000, Quaternary convergent margin tectonics of Costa Rica, segmentation of the Cocos Plate, and Central American volcanism: Tectonics, v. 19, p. 314–334, https://doi.org/10.1029/1999TC001143.

von Huene, R., Ranero, C.R., and Watts, P., 2004, Tsunamigenic slope failure along the Middle America Trench in two tectonic settings: Marine Geology, v. 203, p. 303–317, https://doi.org/10.1016/S0025-3227(03)00312-8.

Vrolijk, P., 1990, On the mechanical role of smectite in subduction zones: Geology, v. 18, p. 703–707, https://doi.org/10.1130/0091-7613(1990)018<0703:OTMROS>2.3.CO;2.

White, R.J., Spinelli, G.A., Mozley, P.A., and Dunbar, N.W., 2011, Importance of volcanic glass alteration to sediment stabilization: Offshore Japan: Sedimentology, v. 58, p. 1138–1154, https://doi.org/10.1111/j.1365-3091.2010.01198.x.

Wiemer, G., and Kopf, A., 2015, Altered marine tephra deposits as potential slope failure planes?: Geo-Marine Letters, v. 35, p. 305–314, https://doi.org/10.1007/s00367-015-0408-4.

Yamano, M., Foucher, J.-P., Kinoshita, M., Fisher, A., and Hyndman, R.D., and ODP Leg 131 Shipboard Scientific Party, 1992, Heat flow and fluid flow regime in the western Nankai accretionary prism: Earth and Planetary Science Letters, v. 109, p. 451–462, https://doi.org/10.1016/0012-821X(92)90105-5.

Yamano, M., Kinoshita, M., Goto, S., and Matsubayashi, O., 2003, Extremely high heat flow anomaly in the middle part of the Nankai Trough: Physics and Chemistry of the Earth, v. 28, p. 487–497, https://doi.org/10.1016/S1474-7065(03)00068-8.

Yue, H., Lay, T., Schwartz, S.Y., Rivera, L., Protti, M., Dixon, T.H., Owen, S., and Newman, A.V., 2013, The 5 September 2012 Nicoya, Costa Rica M_w 7.6 earthquake rupture process from joint inversion of high-rate GPS, strong-motion, and teleseismic P wave data and its relationship to adjacent plate boundary interface properties: Journal of Geophysical Research: Solid Earth, v. 118, p. 5453–5466, https://doi.org/10.1002/jgrb.50379.